Excess Electrons in Polar Solvents*

DAVID A. COPELAND AND NEIL R. KESTNER†
Department of Chemistry, Louisiana State University, Baton Rouge, Louisiana 70803
AND
JOSHUA JORTNER
Institute of Chemistry, University of Tel-Aviv, Tel-Aviv, Israel and *Chemistry Department, James Franck Institute, University of Chicago, Chicago, Illinois 60637*

(Received 3 February 1970)

In this paper we consider a structural model for localized excess electron states in polar solvents with particular reference to dilute metal ammonia solutions and to the hydrated electron. The over-all energetic stability of these species was assessed by considering simultaneously the electronic energy and the medium rearrangement energy. The present model consists of a finite number of loosely packed molecules on the surface of the cavity which are subjected to thermal fluctuations and a polarizable continuum beyond. The electronic energy was computed utilizing an electrostatic microscopic short-range attraction potential, a Landau-type potential for long-range interactions, and a Wigner-Seitz potential for short-range repulsive interactions. The medium rearrangement energy includes the surface tension work, the dipole–dipole repulsion in the first solvation layer, and most importantly the short-range repulsive interactions between the hydrogen atoms of the molecules oriented by the enclosed charge. The gross features of localized electron states in different solvents can be rationalized in terms of different contributions to the medium rearrangement terms. The energetic stability of the localized state of excess electrons in polar solvents was established and the cavity size in the ground state of the solvated electron could be uniquely determined. Experimental energetic and structural data such as volume expansion, coordination numbers, heats of solution, and spectroscopic properties are in qualitative agreement with the predictions of the present model. Optical line shape data calculated from the theoretical model do not agree with experiment; this discrepancy suggests that more data are required in regard to the excited states of the solvated electron.

I. INTRODUCTION

There is currently a wealth of information available on the properties of chemically stable excess electron states in polar solvents (i.e., metal–ammonia solutions, solutions of metals in ammonia and ether)[1–7] and of metastable excess electron states (i.e., electrons in water, alcohols, acetonitrile).[8–14] The physical and chemical properties of dilute metal ammonia solutions and of the hydrated electron, which are assembled in Table I, provide a firm basis for the picture of the solvated electron in polar solvents. These features are independent of the nature of the positive ion, so that in the limit of low concentrations the electron–cation interaction is negligible. The excess electron is expected to be localized by a solvation mechanism which is reminiscent of that of an ordinary ion in an electrolyte solution. The electric field produced by the localized charge distribution of the excess electron polarizes the dipolar solvent molecule, whereupon the nearest-neighbor shell is presumably strongly oriented while the medium outside is subjected to a long-range polarization potential. Adopting this general picture, several theoretical models were proposed to account for the thermochemical and optical properties of the solvated electron. Following early primitive cavity models, the theoretical studies of Deigen,[15] Davydov,[16] and Jortner[17] applied Landau's[18] polaron self-trapping model for the excess electron. Some attempts were also made to account in greater detail for the nature of short-range attractive interaction, which is averaged out in a rather crude manner in the continuum. In an early treatment of this problem the potential was constructed as a superposition of the molecular field of a fixed number ($N=4$) of solvent molecules in the first coordination layer and a continuum contribution beyond it.[19] More recently, Land and O'Reilly[20,21] have constructed a potential due to a finite variable number of polar solvent molecules in the first layer.

Most of these studies were judged in terms of their success in producing "agreement" between theory and experiment. We feel that such criteria are not quite justified in view of the limitation of the crude one-electron scheme employed in all current treatments of the complex quantum mechanical problem of single-electron traps in solids and in polar liquids. At the present stage due to inherent limitations imposed on such one-electron calculations (which we do not hope to improve upon) and the complexity of the physical system, it may be more profitable to focus attention on some general questions pertinent to the physical factors which determine electron localization and the gross features of such a localized state.

The present study of excess electron states in polar solvents was motivated by the impressive progress which was recently achieved in the understanding of excess electron states in nonpolar fluids[22–42] such as He^3, He^4, Ar, Kr, Xe, H_2, and D_2. These studies focused attention on the general problem of the stability of the excess electron state in a liquid, the nature of electron solvent interactions, and the con-

TABLE I. Properties of solvated electrons in water and in liquid ammonia.

Property	System	
	e_{am} (240°K)	e_{aq} (300°K)
$h\nu_{max}$	0.80 eV[a]	1.72 eV[b]
ϵ_{max}	49 000$M^{-1}\cdot cm^{-1}$ [a]	15 800$M^{-1}\cdot cm^{-1}$
Extinction coefficient		
f	0.77[a]	0.65[b]
Oscillator strength		
$W_{1/2}$	0.46 eV[a]	0.92 eV[b]
Half-linewidth		
$dh\nu_{max}/dT$	$-(1.5\pm0.2)\times10^{-3}$ eV/deg[a]	-2.9×10^{-3} eV/deg[b]
ΔH	1.7±0.7 eV[c]	1.7 eV[d]
P	1.6 eV[e]	Unknown
Photoelectric threshold		
Electron mobility	1.08×10^{-2} cm²/V·sec[f]	2.5×10^{-3} cm /V·sec[g]

[a] R. K. Quinn and J. J. Lagowski, J. Phys. Chem. **73**, 2326 (1969).
[b] E. J. Hart and W. C. Gottschall, J. Am. Chem. Soc. **71**, 2102 (1967).
[c] J. Jortner, J. Chem. Phys. **30**, 839 (1959). The uncertainty in this value is due to the (unknown) absolute heat of solvation of the proton in liquid ammonia.
[d] J. H. Baxendale, Radiation Res. Suppl. **4**, 139 (1964). J. Jortner and R. M. Noyes, J. Phys. Chem. **70**, 770 (1966).
[e] G. V. Teal, Phys. Rev. **71**, 138 (1948).
[f] C. A. Kraus, J. Am. Chem. Soc. **43**, 749 (1921).
[g] K. H. Schmidt and W. L. Buck, Science **151**, 70 (1966).

figurational charges in the fluid which may be induced by the presence of an excess electron. Although the properties of excess electrons in nonpolar liquids are somewhat easier to handle by (approximate) theoretical methods, the basic problems involved are identical with those encountered in the study of excess electron states in polar solvents.

The question that should be asked in connection with excess electron states in liquids can be summarized as follows:

(a) *The nature of quasifree and localized excess electron states.* When an excess electron is introduced into a nonpolar or polar liquid, it is not immediately apparent what is the energetically stable state of the electron. The total ground-state energy E_t of the system can be always written in terms of two contributions: the electronic energy E_e and the medium rearrangement energy E_M, so that

$$E_t = E_e + E_M. \tag{1}$$

The second term in Eq. (1) involves the structural modifications induced in the medium due to the presence of the excess electron, so that in general $E_M \geq 0$. The electronic energy has to be computed in the spirit of the Born–Oppenheimer approximation for each nuclear configuration of the medium. In this context two limiting extreme cases should be distinguished:

(1) The quasifree electron state whereupon the excess electron can be described by a plane wave (e.g., a wave packet) which is scattered by the atoms or molecules constituting the dense fluid. Under these circumstances it is expected that the liquid structure is not perturbed by the presence of the excess electron, so that $E_M = 0$. The electronic energy of the quasifree electron state, which we shall denote by V_0, is determined by a delicate balance between short-range repulsions and long-range polarization interactions, so that

$$E_t(\text{quasifree}) = V_0. \tag{2}$$

This energy obviously corresponds to the bottom of the conduction band in the liquid relative to the vacuum level. Theoretical studies based on the Wigner–Seitz model for quasifree excess electron states in nonpolar fluids have established that any dense fluid consisting of molecules which are light and saturated, and thus characterized by a low polarizability, is expected on the basis of pseudopotential theory to exhibit a positive ground-state energy for the quasifree excess electron state.[43] This situation prevails for liquid He, H_2, D_2, and Ne. On the other hand, for heavier rare gases such as Ar, Kr, and Xe the contribution of the attractive long-range polarization overwhelms the contribution of the short-range repulsive pseudopotential, so the $V_0 < 0$ in these systems. Nothing is currently known concerning the V_0 values for polar liquids.

(2) The localized excess electron state where the wavefunction for the excess electron tends to zero at large distances from the localization center. In this case the liquid structure has to be modified to form the localization center. Such a liquid rearrangement process requires the investment of energy. It will be convenient at this stage to specify the configuration of the solvent by a "configurational coordinate" R; the simplest choice is, of course, the mean cavity radius. The total energy of the system can be written

$$E_t(R) = (\text{localized}) = E_e(R) + E_M(R). \tag{3}$$

The most stable configuration of the localized state is obtained by minimizing the total energy [Eq. (3)] with respect to R,

$$\partial E_t(R)/\partial R=0 \qquad \text{at } R=R_0. \tag{4}$$

The resulting energy $E_t(R_0)$ can be, of course, either positive or negative as the liquid rearrangement process requires the investment of energy $[E_M(R_0)>0]$ which is (wholly or partially) compensated by the electronic energy term $E_e(R_0)$.

(b) *The stability of the localized excess electron state.* The absolute sign of the minimum electronic energy of the localized state does not determine whether this localized state will be energetically found. Cases are encountered when $E_t(R_0)>0$ for the localized state [e.g., liquid He where $E_t(R_0)\approx 0.25$ eV] and still the localized state is stable. To assess the energetic stability of the localized excess electron state in a liquid, one has to compare the energy of the localized state with that of the quasifree state. The general stability criterion for the localized state implies that

$$E_t(R_0)<V_0. \tag{5}$$

Following these general considerations, two specific problems have to be considered:

(c) *The nature of electron–solvent interactions.* This general quantum mechanical problem involves the elucidation of the various contributions to the electronic interaction energy of the excess electron in the quasifree and in the localized state.

(d) *Configurational changes in the medium.* In the case of a localized excess electron the liquid structure will be modified because of the following effects:

(1) Local conformational changes arising from short-range electron–solvent repulsion can lead to cavity formation. This effect operates both in nonpolar liquids (e.g., liquid helium) and in polar liquids (e.g., ammonia).

(2) The long-range polarization field induced by the excess electron may lead to marked structural changes in the fluid arising from electrostriction effects, which are operative in both polar and nonpolar liquids, and from the effects of rotational polarization, which are operative in a polar liquid such as water or ammonia.

In order to understand the properties of excess electron states the energy changes accompanying these structural modifications have to be estimated.

In this work we shall consider some of the problems related to the understanding of low-density localized excess electron states in polar liquids where no chemically stable bound states exist for the excess electron. We shall focus attention on the solvated electron in liquid ammonia and in liquid water which provide typical model systems for the localized state in polar solvents. The main theoretical points which will be handled in the present study can be summarized as follows:

(a) *The energy of the quasifree electron state in polar solvents* determines both the stability of the localized state and also the general thermodynamic and optical properties of the solvated electron. Although a reliable theoretical estimate of this energy cannot be provided, we shall present some model calculations which will lead to an "educated guess" of this energy term.

(b) *Energetic stability of the localized state.* Although experiment demonstrates that indeed relation (5) is satisfied in polar solvents, it will be useful to provide a more firm theoretical basis for the stability of the excess electron in polar solvents.

(c) *Configurational stability of the ground state of the solvated electron.* A complete description of the localized state has to involve the calculation of both E_e and E_M. Early studies of the electron cavity model in liquid ammonia introduced the medium rearrangement energy; however, the electronic energy was handled in a rather simplified fashion.[44–46] Later studies based on the polaron model[19] and on a molecular field model[20] were mainly centered on the calculation of the electronic energy at a fixed cavity radius, which was chosen to "fit" the volume expansion data (a "small" value for water and $R_0=3.2$ Å for ammonia). Some contributions of the medium rearrangement energy were introduced at this fixed R_0 to account for thermodynamic properties such as the heat of solution. However, to date no attempt was made to calculate the variation of the total energy accompanied by the change in structural parameters such as the cavity radius or the first-shell coordination number. Nevertheless, some considerations of these terms are to be found in work by O'Reilly[20,47] and, Iguchi.[48] In the present work we shall attempt to establish theoretically the stable configuration of the ground state of the solvated electron by the calculation of the configurational diagrams for the ground state.

(d) *The electronic energy for the cavity model.* We shall consider the following contributions within the framework of the one particle scheme: (1) electronic kinetic energy, (2) short-range repulsions, (3) short-range attractive interactions, (4) long-range attractive polarization interactions. In previous work contributions (3) and (4) were included within the framework of a continuum model. Later a molecular field model was proposed for the short-range attractive interactions. To account for the attractive electronic interactions we shall apply a microscopic molecular electrostatic potential for short-range attractive interactions (3) and a Landau-type polaron potential for the long-range polarization forces (4). The effect of short-range repulsions (2) which was not treated before will be handled by the Wigner–Seitz method

which was successfully applied to localized electron states in nonpolar solvents.

(e) *The medium rearrangement energy.* In the case of nonpolar solvents one has to consider in this context just the contributions of the contractible surface work and the pressure volume work acting on the electron cavity. The situation is much more complicated for polar solvents where the following contributions to E_M have to be considered.

(1) The energy, E_v, required to form a void in the liquid. As in the case of the nonpolar solvents this term can be roughly estimated from the surface tension. Unlike that case, the contribution of this term for polar solvents (where the cavity radius is small) is rather small.

(2) The volume pressure work. This term which is again analogous to that encountered for the nonpolar solvents is important only at high pressures.

(3) The long-range polarization energy π of the medium required for the orientation of the permanent dipoles to form the potential well.

(4) The dipole–dipole repulsion term between E_{dd}, the oriented dipoles in the first coordination layer on the cavity boundary.

(5) Short-range repulsions between the reoriented solvent molecules on the cavity boundary.

(6) The energy required for the rupture of hydrogen bonds.

(f) *Configurational diagrams in excited electronic states.* In spite of the success of previous semiempirical theoretical work to obtain fair agreement with experiment concerning the location of the maximum in the optical absorption of the electron in metal ammonia solutions, many questions remain open. The half-linewidth in the optical absorption amounts to about 60% of the optical excitation energy. The problem of line broadening in the optical spectrum was never properly resolved. These problems will be handled theoretically by calculating the configuration diagrams for the ground and excited electronic states. These configuration diagrams will be then applied for the understanding of the intensity distribution in absorption.

We hope that the present study will provide a better understanding of the structural, thermodynamic, and optical properties of the solvated electron.

II. COMMENTS ON THE ENERGY OF THE QUASIFREE EXCESS ELECTRON STATE IN POLAR SOLVENTS

The energy, V_0, of an excess electron in the bottom of the conduction band of a polar solvent such as ammonia or water is required to establish the energetic stability of the localized ground state and for calculations of the energy levels both in the ground and in the excited states of the solvated electron. As already pointed out, the interaction potential of an electron with a closed-shell atom or molecule in a dense fluid is determined by short-range repulsion and long-range (screened) polarizations interactions. Theoretical studies based on the Wigner–Seitz model[30,33,43] were quite successful in the case of nonpolar solvents, leading to reliable estimates of V_0 values. A similar approach for polar liquids was recently suggested by Cohen and Thompson[49] and by Jortner and Kestner.[50] It will be useful to review briefly this scheme in order to bring up the difficulties involved when it is applied to polar solvents.

Following the work of Cohen, Jortner, and Springett,[33,43] the quasifree electron energy is displayed as a sum of kinetic energy term, T, which accounts for multipole scattering effects, and an attractive interaction, U_p, due to the long-range high-frequency polarization effects. It is important to notice at this point that static or dynamic distortion effects of the liquid are, we assumed, not induced by the quasifree electron, whereupon the long-range polarization field does not contain a contribution from the permanent dipoles which are considered to be randomly oriented. The relevant energetic contributions are

$$V_0 = T + U_p, \tag{6}$$

where the polarization energy is

$$U_p = -(3\alpha e^2/2n_s^4)[(8/7) + (1+8\pi\alpha\rho/3)^{-1}]. \tag{7}$$

α is the polarizability, ρ the liquid density, while $n_s = (3/4\pi\rho)^{1/3}$ corresponds to the Wigner–Seitz radius. The repulsive short-range contribution is given by

$$T = \hbar^2 k_0^2/2m, \tag{8}$$

where m is the electron mass, while the wave vector k_0 is determined from the Wigner–Seitz boundary condition

$$\tan k_0(n_s - \tilde{a}) = k_0 n_s, \tag{9}$$

where the Hartree–Fock short-range potential of the solvent molecule is assumed to be represented by a hard-core radius $\tilde{a}$. In the case of excess electron states in nonpolar liquids the parameter $\tilde{a}$ can be determined from experimental and theoretical electron–atom scattering data.

At this point we encounter the major difficulty in the quantitative application of the present scheme for the quasifree electron states in polar solvents. Gas phase experimental or theoretical electron scattering data cannot be applied for a polar molecule because of the divergence of the dipole term at low energies. We shall attempt to make some rough guesses of the V_0 term applying Eqs. (6)–(9) for a polar solvent such as ammonia. The polarization energy [Eq. (7)] was evaluated by taking $n_s = 2.3$ Å and $\alpha = 2.0 \times 10^{-24}$ cm^{-3}, which leads to $U_p = -3.1$ eV. For the estimate of the T term we feel that as the N–H distance in NH_3 is 1.2 Å while the range of the pseudopotential

associated with the N and H atoms is about 0.5 Å, it is reasonable to take $\tilde{a}\approx 1$ Å. This estimate is consistent with theoretical charge contour data for the NH_3 molecule (see Sec. V). This estimate leads to $T=+3.2$ eV, which leaves us with $V_0=+0.1\pm 1.0$ eV for liquid ammonia. Although this unreliable estimate cannot be taken too seriously, the most important conclusion emerging from the present discussion is that V_0 results from a delicate balance between two large energetic contributions of different signs.

At this disappointing stage of the theoretical development it may be advisable to extract some information on the V_0 terms from experimental data. A lower limit for V_0 can be obtained applying the general stability relation for a localized excess electron state [Eq. (5)] and utilizing the experimental heats of solution of the electron in polar solvents (Table I). Thus $V_0>-1.7\pm 0.7$ eV for NH_3 and $V_0>-1.7$ eV for H_2O.

Unlike the case of nonpolar solvents this value cannot be obtained from adiabatic electron injection experiments since in a polar liquid the dipolar double layer of the solvent molecules absorbed on the electrode will have a large effect on the energetics of the injection process. The best method to determine experimentally the value of V_0 will be provided by photoconductivity and photoemission experiments as V_0 simply corresponds to the energy difference between the thresholds for these two processes. Unfortunately, it is not clear whether a photoemission experiment is feasible.

In view of the large uncertainty in the value of V_0, we shall perform theoretical calculations for the localized state utilizing several physically reasonable values of this energy parameter.

III. MODIFIED CONTINUUM MODELS

As a first step towards a realistic model of a solvated electron in polar solvents, we shall attempt to incorporate short-range interactions into the continuum model for electron medium interactions. In order to calculate the electronic energy in the polaron model, we recall that the Landau potential acting back on the localized electron is given by

$$V(r)=-\beta e^2/R, \qquad r<R,$$
$$V(r)=-\beta e^2/r, \qquad r>R, \tag{10}$$

where $\beta=(D_{op}^{-1}-D_s^{-1})$, D_{op} and D_s correspond to the high-frequency and static dielectric constants, and R is the cavity radius. Until recently the cavity size was introduced as a parameter in the theory. The electronic energy levels E_i in a given electronic state, say i, is given by the sum of the electronic energy, W_i, in the field of the oriented permanent dipoles which exert the potential given by Eq. (10) and the contribution S_i^e of the electronic polarization energy,

$$E_i=W_i+S_i^e. \tag{11}$$

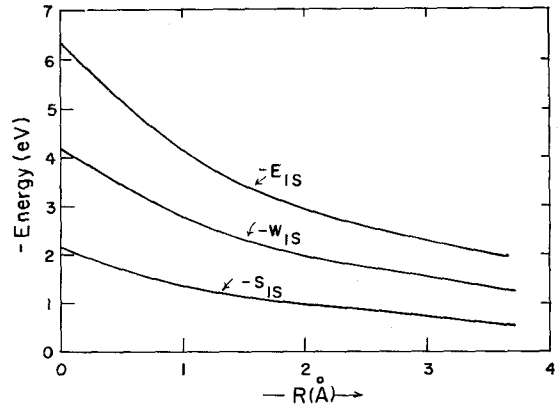

FIG. 1. Ground-state energy contributions for the solvated electron in polar solvents calculated on the basis of the continuum model with $V_0=0$. See Eq. (11).

The energy term W_i is calculated variationally and the mean radius of the charge distribution thus obtained is applied to the calculation of the polarization energy. Many calculations of this type have been reported. For future reference we present in Figs. 1 and 2 the energy terms for the ground $1s$ and the first excited $2p$ state calculated using single-exponent variational wavefunctions. In these calculations it was assumed that $V_0=0$.

In order to account for the effect of short-range repulsions on the electronic levels, we shall now combine the continuum model with the Wigner–Seitz method for the treatment of the localized excess electron state in a polar solvent. The potential acting on the excess electron inside and outside the cavity is taken in the form

$$V(r)=-\beta e^2/R, \qquad r<R,$$
$$V(r)=-\beta e^2/r+V_M, \qquad r>R, \tag{12}$$

where V_M is the potential exerted on the electron by the fluid, which is due to short-range repulsive and long-range polarization interactions. This one-electron potential corresponds to the energy exerted on a quasifree electron which satisfies the eigenvalue equation

$$[-(\hbar^2/2m)\nabla^2+V_M]\phi_0=V_0\phi_0. \tag{13}$$

If pseudopotential theory is invoked at this state, ϕ_0 corresponds to a pseudowavefunction which is "smooth" within the molecular core.

Now the wavefunction $\psi(r)$ for the localized electron inside and outside the cavity can be displayed in the form

$$\psi(r)=f(r), \qquad r<R,$$
$$\psi(r)=f(r)\phi_0(r), \qquad r>R, \tag{14}$$

where outside the cavity the wavefunction for the localized state is modulated by the quasifree electron wavefunction ϕ_0 given by Eq. (13).

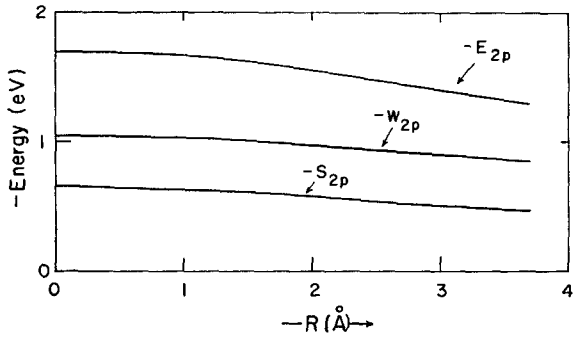

FIG. 2. Energy parameters for the $2p$ excited state of the solvated electron. Continuum model with $V_0=0$. See Eq. (11).

Following the treatment of Springett, Jortner, and Cohen,[43] we now have for the electronic energy

$$[-(\hbar^2/2m)\nabla^2-\beta e^2/R]f(r)=Wf(r), \quad r<R,$$
$$[-(\hbar^2/2m)\nabla^2-\beta e^2/r+V_M]f(r)\phi(r)=Wf(r)\phi(r), \quad r>R. \quad (15)$$

Now neglecting the cross term $[\hat{p}f(R)\hat{p}]\cdot\phi_0(R)$ where $\hat{p}$ is the momentum operator, one immediately obtains

$$[-(\hbar^2/2m)\nabla^2-\beta e^2/R]f(r)=Wf(r), \quad r<R,$$
$$[-(\hbar^2/2m)\nabla^2-\beta e^2/r+V_0]f(r)=Wf(r), \quad r>R. \quad (16)$$

This result is similar to that obtained for the continuum model apart from the incorporation of the V_0 term in the potential outside the cavity. A variational solution of these equations is feasible. This was performed using one-parameter trial wavefunctions for the $1s$ and for the $2p$ states.[50] Calculations performed on the basis of this simple model are summarized in Figs. 3 and 4, where we have displayed pertinent information concerning the ground- and first excited-state charge distributions and the optical excitation energies. From these data it is apparent that:

(a) At a fixed value of R the ground-state electronic energy increases for $V_0>0$ relative to the value for $V_0=0$. Thus in a solvent characterized by a positive V_0 the cavity size will tend to increase in an attempt to reduce this short-range repulsive interaction.

(b) The charge distribution at a given R is pushed into the cavity with increasing V_0.

(c) The energy of the first excited state is more sensitive to short-range repulsive interactions than the ground state. Hence the $1s\rightarrow 2p$ excitation energy at a given R increases with increasing V_0.

These conclusions should be considered only as indicative concerning the role of the short-range repulsive interaction in determining the electronic energy levels. The most important result of the treatment presented in this section involves a realistic way for the introduction of an admittedly crude "coarse graining" method to account for short-range repulsive interactions. However, it should be born in mind that the continuum model for a short- and long-range attractive interaction is rather crude. We shall now attempt to modify the attractive potential. The main advantage of the continuum model is that it introduces a negative constant potential within the cavity. This large constant negative component of the potential is the major factor responsible for the stability of the localized state. We shall now proceed to formulate a more realistic potential field which will include the following ingredients:

(a) An electrostatic microscopic potential will be used to account for short-range attractive interactions due to the oriented solvent molecules in the first coordination layer.

(b) The Landau potential will be retained for long-range attractive interactions exerted by the solvent molecules beyond the first solvation layer.

(c) Short-range interactions will be absorbed into the parameter V_0 as already applied in this section for the continuum model.

The advantages of this modified potential are twofold. In the first place it allows for a more realistic description of the electronic energy levels. Furthermore,

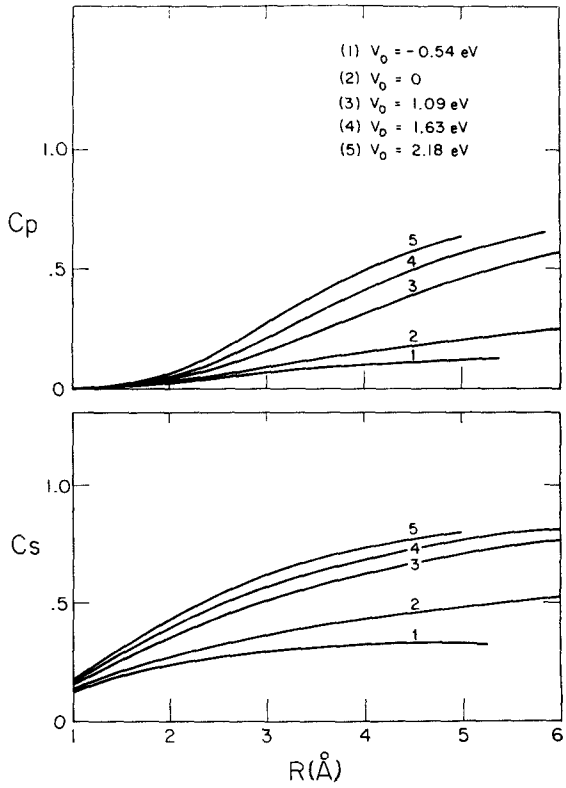

FIG. 3. Charge distributions for the ground and first excited states of the solvated electron for various values of V_0. C_s and C_p represent the fraction of charge confined within radius R for the $1s$ and $2p$ states, respectively, calculated from the modified continuum model.

at a latter stage of the treatment it will be possible to treat in a self-consistent manner the nature of the energy charges accompanying the short- (and long-) range structural modification in the liquid induced by the excess electron. These medium rearrangement energy terms combined with the electronic energy will lead to the *total* energy of the ground and excited states [see Eq. (1)] and will be crucial in determining the ground-state energetic stability and optical properties of the solvated electron.

IV. MOLECULAR MODELS

In the previous section we only considered the nature of the medium in terms of the two parameters β and V_0. No attempt was made to introduce the discrete nature of the medium nor the various molecular parameters of the medium which influence the localization phenomena. Such molecular models are essential if we are to understand all features of the experimental results, especially the variations in properties between different solvents.

Since the theory of liquids is not sufficiently advanced that we can consider the entire system of an electron plus a large number (about Avogadro's number) of molecules, we must construct models which begin to mimic real situations in part. In a manner similar to the theory of electrolyte solvation, we assume that around each electron are a small number, N, of symmetrically distributed solvent molecules which constitute a first solvation layer. Beyond that we have little choice but to assume the solvent is a continuum. Each of these N solvent molecules has a dipole moment (assumed to be at its center), is of finite size (see the next section for details), and has an isotropic polarizability. Any specific effects of electron solvent molecule interaction beyond the first layer are expected to be smaller since the molecules are further removed and subject to the dielectric screening of the closer molecules.

The specific electron–medium potential responsible for electron localization is now subdivided into short-range attractive interactions, long-range polarization

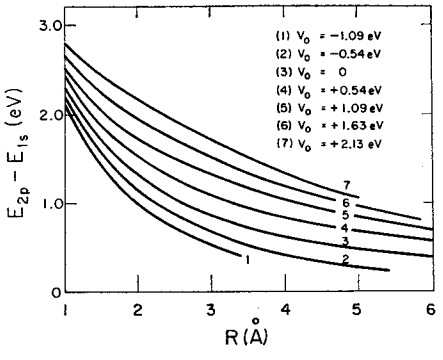

FIG. 4. The dependence of the $1s \rightarrow 2p$ excitation energy on V_0 for the modified continuum model.

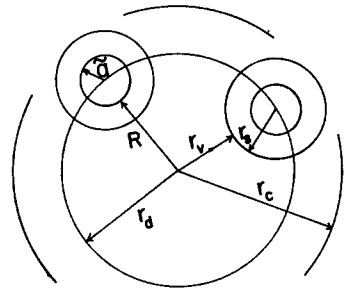

FIG. 5. Definitions of the distances involved in the molecular models. r_v is the void radius of the cavity, r_s the effective solvent radius, and $\tilde{a}$ is the effective hard core of the molecules located a distance r_d from the center of the cavity. The continuum begins at r_c.

interaction, and short-range repulsive terms. Using the assumptions outlined above, the interaction takes the following form:

$$V(r) = -N\mu e/r_d^2 - \beta e^2/r_c, \qquad r < R,$$
$$= -\beta e^2/r + V_0, \qquad r > R, \qquad (17)$$

using the notation described in Fig. 5. μ is the effective dipole moment of the molecule, a concept to be discussed later. The radius r_d is the distance from the center of the cavity to the center of the molecule (and thus to the dipole), while r_c is the distance from the center of the cavity to the beginning of the continuum beyond the first layer. We assume here that polarization effects are not primarily responsible for localization and can be added later.

The first term in Eq. (17) is the charge dipole interaction based on a unit charge localized at the center of the cavity. The energy contribution of this term is only proportional to the charge enclosed. Also included in this term is an effective dipole moment, μ. The interaction depends on the product of the value of μ_0, the actual dipole moment of the molecule times the average value of the cosine of the angle between the dipole moment vector and the radius vector,

$$\mu = \mu_0 \langle \cos\theta \rangle. \qquad (18)$$

We shall assume that μ_0 is the gas phase dipole moment. The average value of the cosine depends on two major factors: temperature and the strength of the orienting electric field. We shall use the Langevin function to express this relationship,

$$\langle \cos\theta \rangle = \coth\chi - 1/\chi, \qquad (19)$$

where $\chi = \mu_0 E_{\text{loc}}/kT$ and $E_{\text{loc}} = eC_i/r_d^2$. The local electric field, E_{loc}, contains a variable C_i which is the amount of charge enclosed in the region 0 to R since this charge determines the magnitude of the orienting field and for a spherical distribution can be simply placed at the center of the cavity. This charge must be determined by a self-consistent procedure. In using the Langevin factor, we have assumed that orientation of the dipoles in the first layer is dominated by the enclosed charge and only slightly affected by other factors. In considering molecules farther removed from the cavity, E_{loc} is decreased and other factors

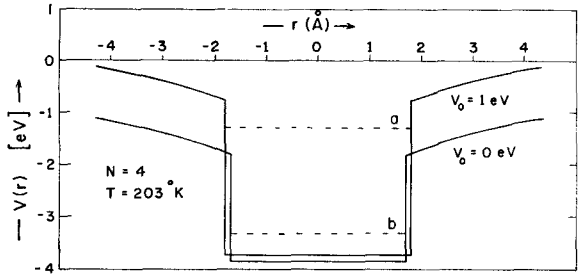

FIG. 6. The potential (self-consistently calculated) which traps the electron in the cavity for two values of V_0 and four molecules in the first layer. Line a represents the depth of the potential obtained from the continuum model for $V_0=0.0$ and $R=3.2$ Å. Line b represents the continuum model's potential depth for $V_0=0.0$ and $R=1.7$ Å, corresponding to the R_0 of the molecular case.

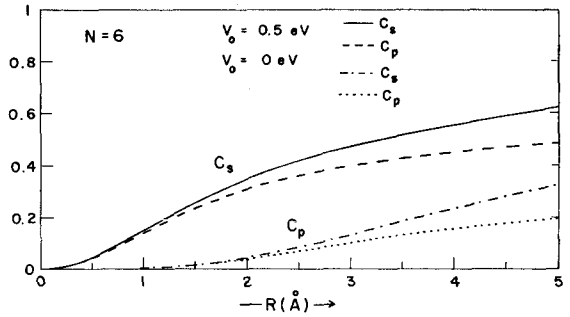

FIG. 8. Charge enclosed in a sphere of radius R for the $1s$ (represented as C_s) and for the $2p$ (represented as C_p) states in the molecular model.

are important in orientation, supporting our assumption that the continuum can be introduced via the simple Landau potential.

In defining the parameters pertaining to the ammonia molecules, we have used the following (see Fig. 5):

$$R=r_v+r_s-\tilde{a}_s, \tag{20}$$

where r_s is the radius of the solvent molecule while $\tilde{a}_s$ corresponds to the "hard-core" repulsive parameter, and r_v is the actual void radius. It is reasonable to take $\tilde{a}_s\sim 1$ Å for ammonia since inspection of the theoretical charge contour data calculated using a limited basis set SCF scheme leads to a value of about 0.98 Å. The average radius of the ammonia molecule in the unperturbed liquid was estimated to be 2.3 Å. The zero point of the Lennard-Jones potential for NH_3 is considered to be about 1.7 Å. Because electrostriction affects the close contact between solvent molecules on the cavity boundary, we will choose $r_{NH_3}\sim 1.5$ Å. The center of the closest solvent molecule from the center of the cavity is then taken to be

$$r_d=r_v+r_s=r_v+1.5. \tag{21}$$

These choices primarily affect only the continuum contributions.

The electronic energy of the ground and excited state are determined by substituting one-parameter Slater $1s$ and $2p$ functions and minimizing the energy with respect to those parameters. We denote A as the $1s$ exponent and D as the $2p$ exponent.

Using the potential in Eq. (17), we obtain an energy W_i which for the ground ($1s$) state is

$$W_{1s}=\tfrac{1}{2}A^2-(Ne\mu_0\langle\cos\theta\rangle/r_d^2+\beta e^2/r_c)C_s$$
$$+V_0(1-C_s)-\int_{r=R}^{r=\infty}\phi_{1s}^*\left(\frac{\beta e^2}{r}\right)\phi_{1s}d\tau, \tag{22}$$

where $d\tau$ is the volume element and C_s, the charge enclosed, is

$$C_s=\int_{r=0}^{r=R}\phi_{1s}^*\phi_{1s}d\tau. \tag{23}$$

Equation (22) must be solved self-consistently since the cosine term depends on C_s and thus on ϕ_{1s} (or A) also. One simply requires a good initial guess of $\langle\cos\theta\rangle$ and a few iterations to achieve quick solutions.

The energy of the first excited state is found from an equation similar to Eq. (22) with ϕ_{1s} replaced by ϕ_{2p} and C_s replaced by C_p:

$$C_p=\int_{r=0}^{r=R}\phi_{2p}^*\phi_{2p}d\tau, \tag{24}$$

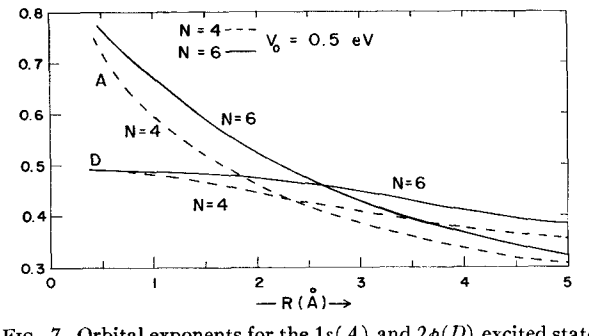

FIG. 7. Orbital exponents for the $1s(A)$ and $2p(D)$ excited states for two values of N and $V_0=0.5$ eV.

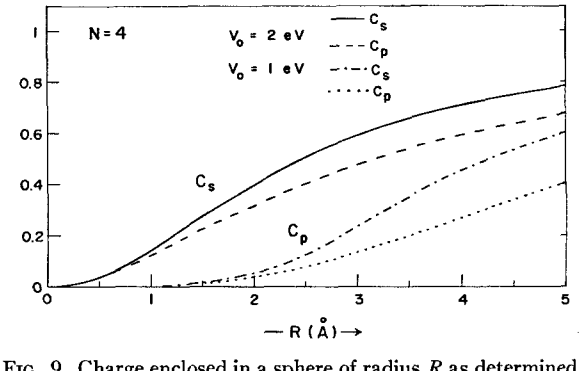

FIG. 9. Charge enclosed in a sphere of radius R as determined by the molecular model for $N=4$ and $V_0=1$ and 2 eV.

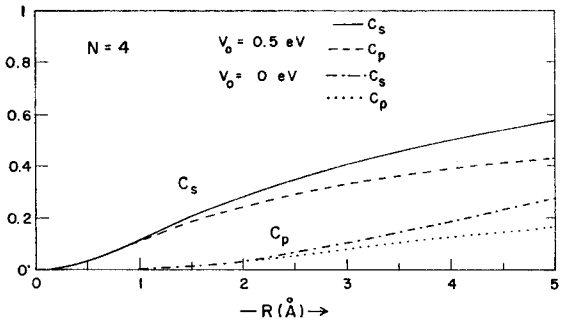

FIG. 10. Charge enclosed in a sphere of radius R as determined by the molecular model for $N=6$ and two values of V_0.

namely,

$$W_{2p}=\tfrac{1}{2}D^2-(Ne\mu_0\langle\cos\theta\rangle_{1s}/r_d^2+\beta e^2/r_c)C_p$$
$$+V_0(1-C_p)-\int_{r=R}^{r=\infty}\phi_{2p}^*\left(\frac{\beta e^2}{r}\right)\phi_{2p}d\tau, \quad (25)$$

where it is most important to realize that the average value of the cosine is that calculated for the ground or $1s$ state. No self-consistent procedure is involved in solving Eq. (25) since the potential is determined by the ground electronic configuration. This is the appropriate state to use in the present calculation since excitations occur so rapidly that the medium is not allowed to rearrange.

The total electronic energy must include the electronic polarization contributions[51]

$$E_i=W_i+S_i, \quad (26)$$

where

$$S_i=-\frac{N\alpha C_i^2}{r_d^4}-\tfrac{1}{2}(e\gamma_0)\int_R^\infty\left(\int_{r=0}^r\phi_i^2d\tau\right)^2\frac{dr}{r^2}, \quad (27)$$

with ϕ_i being either the $1s$ or $2p$ function and

$$\gamma_0=1-1/D_{op}. \quad (28)$$

The first term on the right is the electronic polarization of the molecules on the surface of the cavity. The remaining term arises from the polarization of the continuum and is similar to the electronic polarization contributions of the modified continuum model (Sec. III).[51]

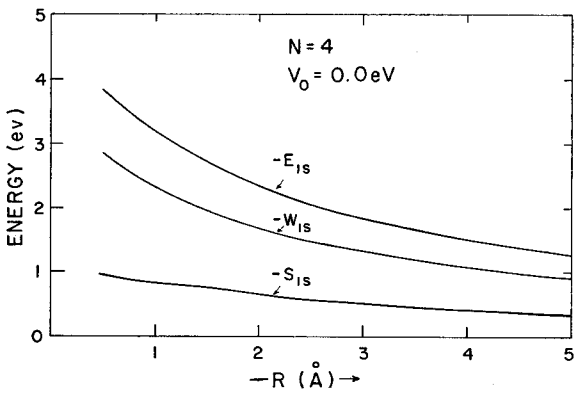

FIG. 11. Electronic energy contributions for the ground state as obtained in the molecular models for $V_0=0.0$ and $N=4$. This should be compared with Figs. 1 and 12.

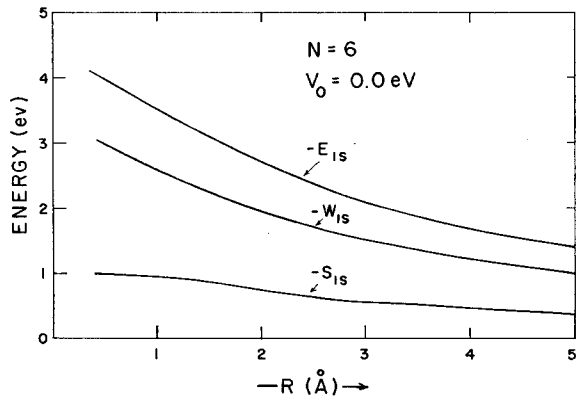

FIG. 12. Electronic energy contributions for the ground state as obtained in the molecular models for $V_0=0.0$ and $N=6$. This should be compared with Figs. 1 and 11.

The "exact" value of V_0 is not known (although it is not expected to be far from $V_0\approx 0$); also, the best value of N to use is not obvious. Thus we decided to perform calculations for various values of N. We selected 4, 6, 8, and 12 as representative values based on the liquid density and other considerations. The particular numbers selected were dictated by the ease of calculating the medium reorganization energy, which will be discussed in the next section.

In Fig. 6 we present two typical self-consistently calculated potentials [Eq. (17)] for $N=4$. Note how insensitive the depth is with regard to V_0. In Fig. 7 we show the best $1s$ and $2p$ orbital exponents for $N=4$ and $N=6$ at one value of V_0 as a function of the cavity size. The plots of charge enclosed as a function of R for both the ground and excited states are shown in Figs. 8–10. Figures 11–14 represent the various contributions to the electronic energy for typical cases. These should be compared with the original and modified continuum theory (Figs. 1–4),

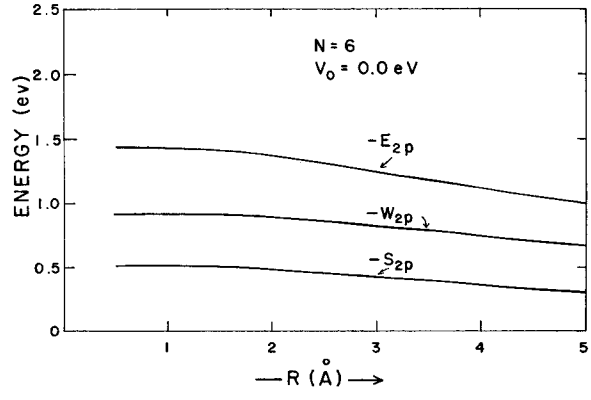

FIG. 13. Electronic energy contributions for the first excited state as determined by molecular models for $V_0=0.0$ and $N=6$. This should be compared with the continuum results in Fig. 2.

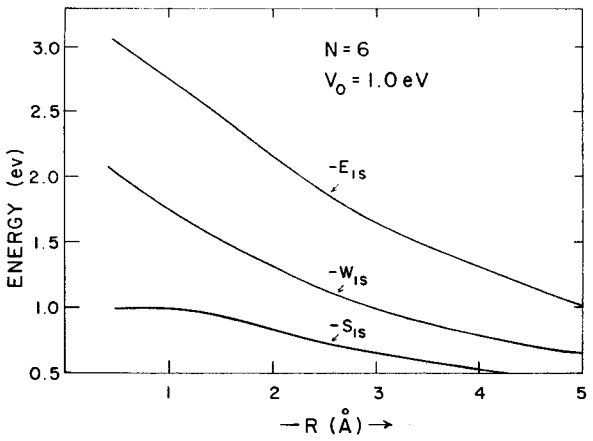

FIG. 14. Ground-state electronic contributions as determined by the molecular model for $N=6$ and $V_0=1.0$ eV. This should be compared to the corresponding results for $V_0=0.0$ in Fig. 12.

as there are many similarities especially for $N=6$. It is found that for $N=6$ actual calculations of the self-consistent potential inside the cavity are within 10% of those of the continuum model if R is the same in both cases and of typical values 1–3 Å. The $N=4$ case has a higher energy while N values larger than 6 are much lower than the predictions of the continuum result. Also in Fig. 6 we show the con-

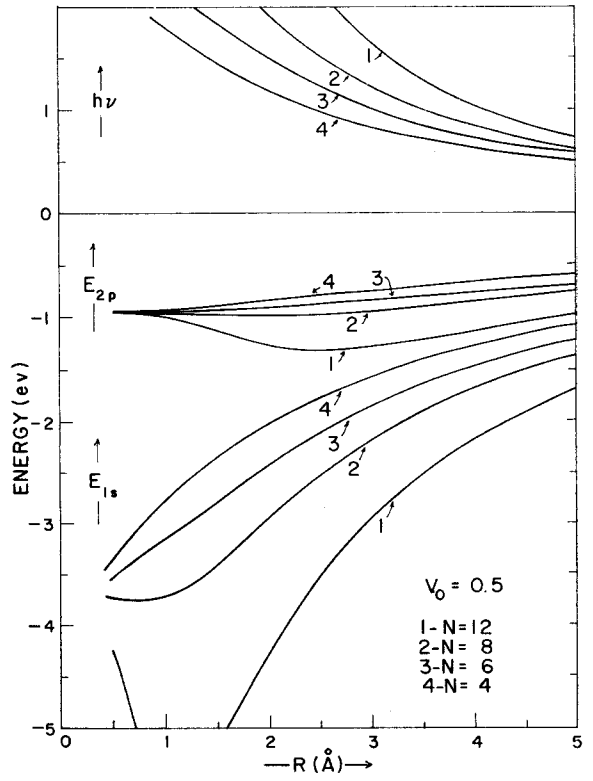

FIG. 15. Total ground-state electronic energy (E_{1s}), total excited state electronic energy (E_{2p}), and the excitation energy, $h\nu$, as determined by the molecular model as a function of the cavity size, R, for $V_0=0.5$.

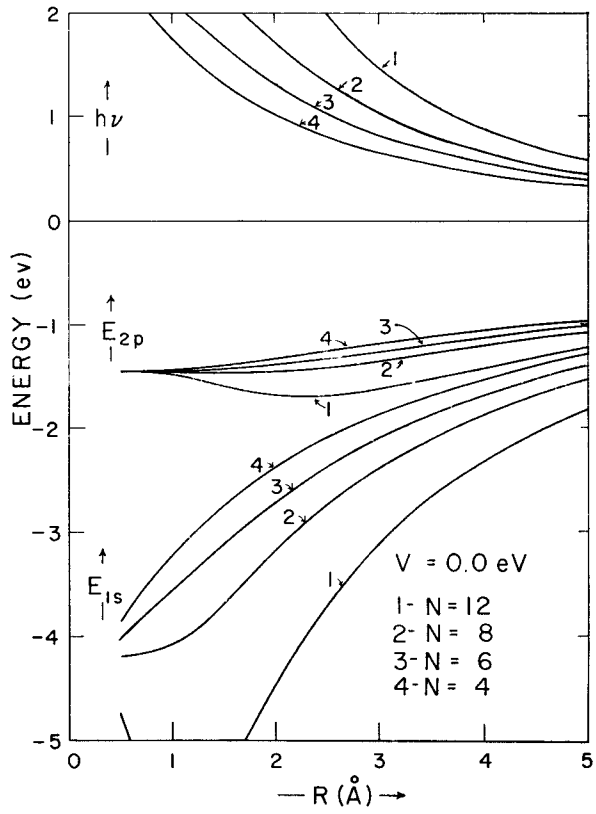

FIG. 16. The same quantities as in Fig. 15 for $V_0=0.0$.

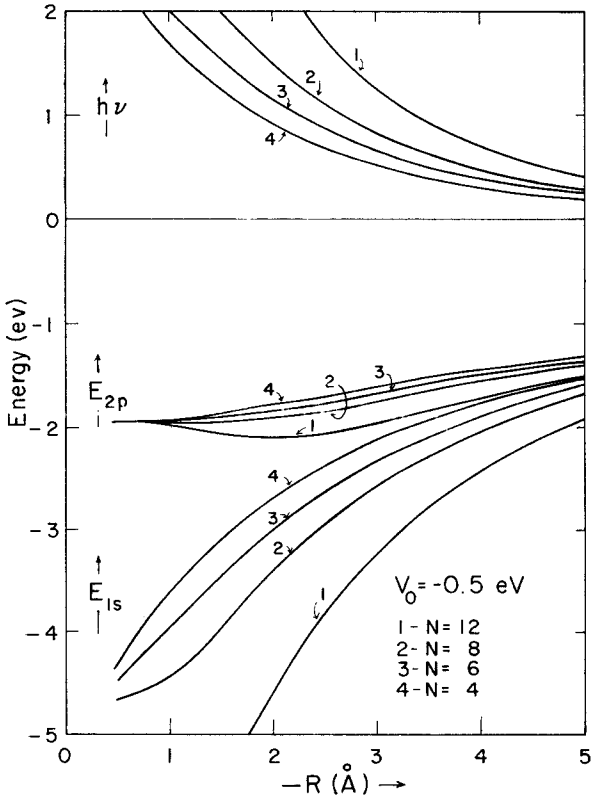

FIG. 17. The same quantities as in Fig. 15 for $V_0=-0.5$.

tinuum predictions inside the cavity for $V_0=1$ eV and the two values of R, namely, 3.2 (the value used in early calculations[17]) and 1.70 Å, a value more appropriate based on the present calculations.

More complete plots of the total electronic energy and the excitation energy ($E_{2p}-E_{1s}$) for several values of V_0 are shown in Figs. 15–17. These numbers are not useful in themselves as they indicate only energies versus R and say nothing about the correct cavity size to use. We must consider in addition the factors which uniquely determine R, and to do so, we need to study the detailed interactions of the medium molecules. After having done this, we can present more complete data on the various parameters at their stable configurations. The important point is that for $N=4$ and 6 the transition energy $h\nu=E_{2p}-E_{1s}$ is of a reasonable magnitude to agree with the experimental data. The unique value will be found in the next section.

V. MEDIUM REARRANGEMENT ENERGY

The calculations of the preceding two sections considered only one aspect of the changes in the solvent when the electron was introduced. We have not considered the energy changes of the solvent–solvent molecule interactions induced by the electron. However, we assumed that the electron oriented those molecules in the first solvation layer and polarized the solvent beyond it, and that these configurational modifications must lead to some major energetic contributions. In fact, without worrying about such a contribution, the lowest energy state for the electron would be in a cavity of zero size in most cases.

Let us now consider what happens to solvent–molecule interactions in the first layer when an elec tron is introduced. Imagine the following process:

(a) We create a cavity of size R.

(b) We introduce a charge with a distribution given by the problem considered in the previous section.

(c) The molecules are now allowed to rotate under the field of the trapped electron. This leads to changes in molecule–molecule interactions.

(d) The continuum outside the first solvation layer is readjusted in the field of the charge distribution.

The energy of the first process can be approximated by the surface tension

$$E_{ST}=4\pi\gamma R^2, \tag{29}$$

where $\gamma\cong 40$ dyn/cm.

There is another term which should be included in the first step, namely, the energy to create a void of volume V against an external pressure,

$$E_{pv}=\tfrac{4}{3}\pi R^3 P, \tag{30}$$

but this is exceedingly small for the cases we consider here, i.e., pressures around normal atmospheric pressure. Only if the pressure were increased greatly would this factor be of any interest at all. One example of such a case is the stability of localized electrons in solid helium considered by Cohen and Jortner.[52]

When the molecules in the first solvation layer adjust under the influence of the enclosed charge, two things happen. First, since the dipoles are all pointed in a similar direction (to a large extent), there will be a net electrostatic repulsion between neighboring dipoles relative to the "almost" random array which occurs in the liquid in the absence of an extra charge. In addition, in molecules such as ammonia and to a lesser extent water and other molecules with two hydrogens, when the dipole moment is oriented, hydrogen–hydrogen distances between neighboring molecules are decreased since all hydrogens are now forced to point forward. This leads to hydrogen–hydrogen repulsions, which also increase the medium rearrangement energy.[53]

The repulsion of dipoles and the hydrogen–hydrogen interactions can only be handled with ease for certain coordination numbers of first-neighbor molecules, namely, 4, 6, 8, and 12. Larger values of N were not considered, as close packing of such a large number of solvent molecules in the first layer is physically unsound. This conclusion is supported by the trends observed in our calculations. For the dipole–dipole interactions of these interactions, we have a contribution of the form

$$E_{dd}=D_N\mu_T^2/r_d^3, \tag{31}$$

where D_N is a numerical constant which depends on the number of molecules in the first layer. Using the constants from a paper by Buckingham,[54] we have

$$\begin{aligned} D_4&=2.2964,\\ D_6&=7.1140,\\ D_8&=12.820,\\ D_{12}&=41.074. \end{aligned} \tag{32}$$

The dipole moment which is to be used in Eq. (13) is the total dipole moment along the radius vector including that induced by the charge enclosed:

$$\mu_T=\mu_0\langle\cos\theta\rangle+e\alpha C_s/r_d^2, \tag{33}$$

where α is the (assumed) isotropic polarizability of the ammonia molecule and C_s is the charge enclosed in the ground state [Eq. (23)]. The components of the dipole moment in other directions do not contribute to the dipole–dipole repulsion energy.[55]

The hydrogen–hydrogen repulsions must be estimated from a rather specific model. The hydrogen–hydrogen interaction judged best by Eisenberg and Kauzman from their studies on water[56] was

$$\phi_{H-H}=434\exp(-4.60r_H)\quad(\text{eV}). \tag{34}$$

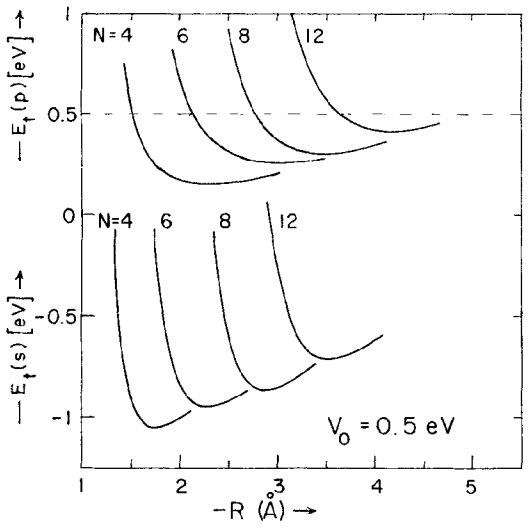

FIG. 18. The total energy (electronic plus medium reorganization) of the ground state $E_t(s)$ and the first excited state $E_t(p)$ for the molecular model as a function of cavity size for $V_0=0.5$.

In each case the total repulsion is related to N by some numerical factor (being careful to avoid double counting). The distance between hydrogens, r_H, must be studied carefully. Using charge densities of Bader and Jones,[57] one finds that the hydrogens lie in a plane about $R+0.58$ Å with a radius of about 0.93 Å. Since the hydrogen's are somewhat free to rotate to reduce their repulsions, we assumed that the effective radius of the hydrogens was somewhat less than 0.93 Å, namely, 0.71 Å, based on charge density plots. This factor is difficult to determine more accurately.

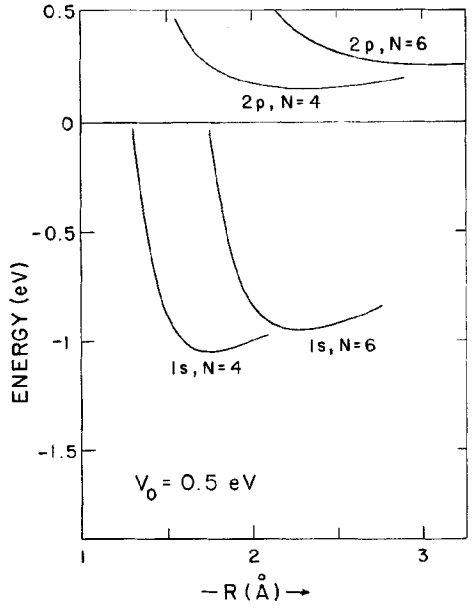

FIG. 19. The total energy of the ground and first excited state, an expanded version of Fig. 18 for $V_0=0.5$ and $N=4$ and 6.

With the above choices the total hydrogen–hydrogen repulsion can be expressed in the following form:

$$E_{HH}=C_{HH}^{(N)}\exp[-4.60(A_N R-B_N)], \quad (35)$$

where the constants depend on the geometry and are listed in Table II.

As mentioned in the Introduction, there is an additional contribution due to the solvent molecules, namely, the energy to rupture hydrogen bonds. In our discussions of ammonia as the solvent we have neglected this contribution. Introduction of the effects of such terms as a barrier to rotation did not change our results significantly, and thus we have neglected its effect for the present. Because the hydrogen bonding is weak in ammonia, we believe this is a small contribution, but it may not be small in other solvents such as water (see Sec. IX). In addition we have neglected all higher multipole interactions between molecules.

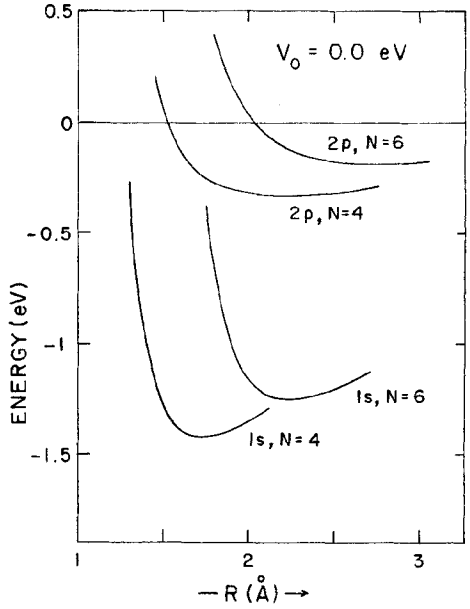

FIG. 20. The total energies of the ground and first excited states for the molecular model with $V_0=0.0$.

Finally, we have a fourth contribution, namely, the effect of the electron on the continuum. Using the formula originated by Jortner[17] and corrected by Land and O'Reilly,[20] we have

$$\pi=\tfrac{1}{2}\beta\left(\int_{r_c}^{\infty}G_0(r)\phi_{1s}{}^2r^2dr+G_0(r_c)P(r_c)\right), \quad (36)$$

where

$$G_0(r)=r^{-1}\int_0^r|\phi_{1s}(s)|^2s^2ds+\int_r^{\infty}|\phi_{1s}(s)|^2sds \quad (37)$$

and

$$P(r_c)=e\int_0^{r_c}|\phi_{1s}(s)|^2 s^2 ds. \quad (38)$$

This represents the average interaction of the medium to the enclosed charge in the same spirit as the original continuum model.

The numerical values of these various terms will be summarized later in the paper for the most stable configurations. From the form of the terms we see that very small cavities are characterized by a very large rearrangement energy *if* the dipoles can be oriented or equivalently if a large amount of charge can be enclosed. From various numerical studies with varying conditions we have confirmed this conclusion. Even an introduction of a reasonable barrier to rotation did not change seriously the fact that most molecules are oriented with their hydrogens pointing inward. For large cavity sizes the hydrogen–hydrogen repulsion contribution decreases rapidly and the dipole–dipole repulsion dominates, and for a constant coordination number this contribution decreases as the inverse cube of the cavity radius.

VI. CONFIGURATIONAL STABILITY

In the original work on the continuum model[17] and even in the modified version for the interaction potential presented in Sec. II of this paper no prediction is made of the existence or stability of the cavity model. Obviously the electronic energy increases as the cavity size decreases. Thus, unless the medium rearrangement energy is introduced, one cannot predict the size of the energetically stable cavity. In some preliminary work published in Ref. 50, we made a first attempt in this direction. The present paper contains a more thorough analysis of the configurational stability.

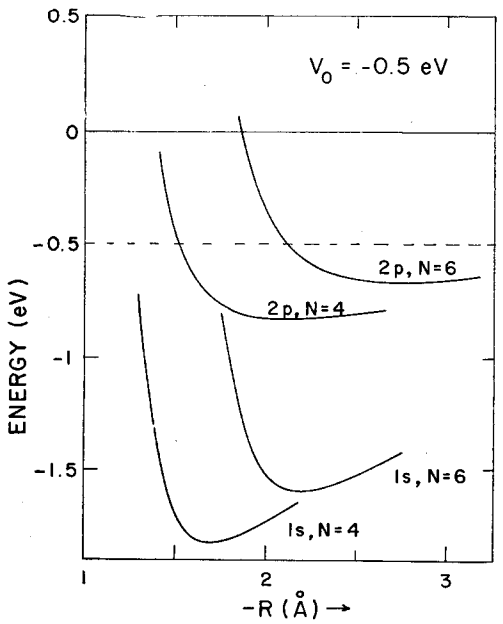

FIG. 21. The total energies of the ground and first excited states of the molecular model for $V_0=-0.5$.

TABLE II. Constants representing the hydrogen–hydrogen repulsions [See Eq. (16)].

Molecules in first layer N	$C_{HH}^{(N)}$ (eV)	A_N (Å^{-1})	B_N (Å)
4	2 602.4	1.633	0.471
6	5 204.7	1.155	0.752
8	6 940.0	1.155	0.752
12	10 416.0	1.000	0.843

To predict the stability of the electron cavity, one needs to show that the *total* energy of the system, i.e., electron plus medium [Eq. (1)], is a minimum for a finite radius. One can not, therefore, consider either the electronic or the medium energy separately.

Unless we consider the entire process of the solution of, say, sodium metal in liquid ammonia, we can not predict the absolute stability of finding solvated electrons and solvated sodium ions in ammonia solutions. We can, however, predict the state of the electron. The electron is localized if Eq. (5) applies, namely, if the total energy is less than the energy of a quasifree electron. The continuum model or the molecular model based solely on the electronic energy could always be made to satisfy Eq. (5) by choosing R small enough. This, however, does not uniquely define a cavity model since R_0, the cavity radius, can be arbitrarily selected to agree with one or more experimental data such as optical excitation energies.

One could try to amend the continuum model by appending to it a medium reorganization which corresponds to the work required to polarize a continuum dielectric. Such a simple procedure does predict that the stable configuration corresponds to $R=0$. One could proceed one step further and combine the electronic energy calculated on the basis of the continuum model (Sec. III) with the medium rearrangement energy calculated by a molecular model (Sec. V). Such an approach was previously adopted by us.[50] However, we feel that this is an inconsistent procedure since the medium energy must be computed for a finite number of molecules in the first layer, and it is therefore essential to consider a molecular model both for the medium rearrangement energy *and* for the electron medium interaction potential. For this stable configuration the energy expressed in terms of the configurational coordinate R must be a minimum,

$$(\partial E_t/\partial R)_{R_0}=0$$

and

$$(\partial^2 E_t/\partial R^2)_{R_0}>0. \quad (39)$$

We do not know the exact value of V_0 nor of N;

TABLE III. Electronic energy results for the most stable molecular cavity models at $T=203°K$.[a]

		Ground state				Excited state			Transition energy	Estimated half-width[b]
V_0	R_0 (Å)	A (Å^{-1})	W_{1s}	S_{1s}	E_{1s}	D(Å^{-1})	W_{2p}	E_{2p}	$h\nu$	Δ_e
$N=4$										
2.0	2.00	0.568	−0.3724	−0.7863	−1.1587	0.503	1.0520	0.5293	1.6879	0.17
1.5	1.85	0.544	−0.7124	−0.7766	−1.4890	0.480	0.5804	0.0740	1.5630	0.13
1.0	1.80	0.514	−1.0681	−0.7522	−1.8203	0.466	0.0967	−0.3976	1.4223	0.13
0.5	1.75	0.487	−1.4496	−0.7294	−2.1790	0.456	−0.3913	−0.8762	1.3028	0.12
0.0	1.72	0.460	−1.8421	−0.7053	−2.5474	0.448	−0.8826	−1.3550	1.1924	0.12
−0.5	1.70	0.435	−2.2466	−0.6816	−2.9282	0.439	−1.3723	−1.8410	1.0872	0.13
$N=6$										
2.0	2.50	0.582	−0.6822	−0.8070	−1.4892	0.591	0.8996	0.3297	1.8189	0.26
1.5	2.40	0.556	−0.9307	−0.7948	−1.7255	0.539	0.4913	−0.0485	1.6770	0.21
1.0	2.35	0.524	−1.1989	−0.7662	−1.9651	0.499	0.0488	−0.4636	1.5015	0.21
0.5	2.25	0.495	−1.5175	−0.7436	−2.2611	0.470	−0.4112	−0.9025	1.3586	0.16
0.0	2.25	0.455	−1.8233	−0.6995	−2.5228	0.448	−0.8828	−1.3559	1.1728	0.15
−0.5	2.20	0.422	−2.1785	−0.6654	−2.8439	0.428	−1.3573	−1.8121	1.0319	0.14
$N=8$										
2.0	3.00	0.570	−0.9348	−0.7793	−1.7141	0.657	0.6191	0.0180	1.7321	0.24
1.5	2.95	0.545	−1.1189	−0.7648	−1.8837	0.605	0.2949	−0.2755	1.6082	0.21
1.0	2.90	0.516	−1.3261	−0.7439	−2.0700	0.550	−0.0696	−0.6063	1.4637	0.18
0.5	2.85	0.483	−1.5593	−0.7157	−2.2750	0.499	−0.4704	−0.9728	1.3021	0.16
0.0	2.85	0.440	−1.7973	−0.679	−2.4674	0.452	−0.8964	−1.3638	1.1035	0.14
−0.5	2.80	0.400	−2.0880	−0.6288	−2.7168	0.417	−1.3439	−1.7830	0.9338	0.14
$N=12$										
2.0	3.60	0.555	−1.3541	−0.7562	−2.1103	0.691	0.0986	−0.5330	1.5774	0.23
1.5	3.60	0.532	−1.4723	−0.7377	−2.2100	0.651	−0.1307	−0.7339	1.4761	0.23
1.0	3.55	0.510	−1.6268	−0.7272	−2.3540	0.609	−0.3889	−0.9640	1.3900	0.20
0.5	3.55	0.478	−1.7738	−0.6982	−2.4720	0.555	−0.6827	−1.2187	1.2533	0.19
0.0	3.50	0.446	−1.9665	−0.6725	−2.6390	0.500	−1.0189	−1.5165	1.1225	0.17
−0.5	3.50	0.402	−2.1555	−0.6249	−2.7804	0.439	−1.3917	−1.8418	0.9386	0.16

[a] All energies in electron volts.
[b] Half-width estimated by range of $h\nu$ included within a variation of $E_t(1s)$ by kT, where k is Boltzmann's constant [see Eq. (56)].

thus calculations were performed for various values of these parameters. Typical plots for $V_0=0.5$ are shown in Fig. 18. The results for $N=4$ appear to be most stable for this and all other V_0 values studied. However, the difference in energy between the four, six, and even the eight molecule cavities are probably within the limitations of this method. This leads one to suspect that there may be present in solution cavities of various sizes and various coordination numbers of molecules in the first layer. The most important result of this plot and all other results obtained in this study is that there exists a stable cavity species of a radius R in the region 1.70 Å to about 2.2 Å. This number is below that usually quoted based on volume expansion data but is not directly comparable for reasons we will discuss later. In Tables II and III we summarize the various energetic contributions which lead to the results obtained at 203°K for various N and V_0 values. In Figs. 19–21 the effect of V_0 is presented in more detail for the $N=4$ and $N=6$ cavities.

We have not listed detailed values for the charge enclosed in the cavity. In some cases these can be obtained from earlier figures. The amount of charge increases for larger V_0 and larger N because both effects favor greater stability. Typical values at the equilibrium configurations are given in Table IV. These values are roughly 10%–15% higher than those obtained from the simple polaron continuum model at the same value of R.

Finally, for later reference we present values for the $N=4$ and 6 cases of the calculations when the temperature is increased to 300°K in Table V. These are calculated by simply changing the temperature and the dielectric constants.

VII. GROUND-STATE PROPERTIES

The theoretical calculations for the ground state of the solvated electron in dilute metal ammonia solutions suggest that for reasonable V_0 values in the range +0.5 to −0.5 eV the energetically stable configuration of the ground state is characterized by a

TABLE IV. Medium and total energy results for the most stable molecular cavity models at $T=203°K$.[a]

V_0	R_0 (Å)	E_{dd}	E_{et}	E_{HH}	π	$\langle\cos\theta\rangle$	$E_t(1s)$	$E_t(2p)$
$N=4$								
2.0	2.00	0.1745	0.1256	0.0068	0.8023	0.909	−0.0495	1.6215
1.5	1.85	0.1912	0.1075	0.0209	0.8168	0.901	−0.3525	1.2105
1.0	1.80	0.1877	0.1017	0.0305	0.8123	0.889	−0.6881	0.7346
0.5	1.75	0.1628	0.0962	0.0444	0.8058	0.876	−1.0486	0.2542
0.0	1.72	0.1816	0.0928	0.0556	0.7981	0.861	−1.4293	−0.2369
−0.5	1.50	0.1667	0.0907	0.0646	0.7791	0.843	−1.8269	−0.7396
$N=6$								
2.0	2.50	0.3456	0.1963	0.0071	0.7360	0.912	−0.2042	1.6147
1.5	2.40	0.3644	0.1809	0.0137	0.7447	0.907	−0.4219	1.2551
1.0	2.35	0.3606	0.1734	0.0189	0.7436	0.900	−0.6686	0.8329
0.5	2.25	0.3724	0.1590	0.0362	0.7470	0.880	−0.9465	0.4120
0.0	2.25	0.3411	0.1590	0.0362	0.7307	0.876	−1.2557	0.0830
−0.5	2.20	0.3269	0.1520	0.0502	0.7183	0.856	−1.5969	−0.5647
$N=8$								
2.0	3.00	0.4234	0.2826	0.0264	0.6741	0.904	−0.3076	1.4245
1.5	2.95	0.4385	0.2733	0.0344	0.6768	0.900	−0.4707	1.1375
1.0	2.90	0.4293	0.2641	0.0449	0.6778	0.893	−0.6539	0.8098
0.5	2.85	0.4242	0.2550	0.0586	0.6761	0.886	−0.8611	0.4410
0.0	2.85	0.3913	0.2550	0.0586	0.6634	0.871	−1.0991	0.0045
−0.5	2.80	0.3706	0.2462	0.0764	0.6509	0.851	−1.3727	−0.4389
$N=12$								
2.0	3.60	0.7528	0.4069	0.0324	0.6112	0.889	−0.3070	1.2704
1.5	3.60	0.7359	0.4069	0.0324	0.6094	0.885	−0.4254	1.0508
1.0	3.55	0.7470	0.3957	0.0407	0.6119	0.882	−0.5587	0.8313
0.5	3.55	0.7180	0.3957	0.0407	0.6079	0.874	−0.7097	0.5436
0.0	3.50	0.7110	0.3847	0.0513	0.6064	0.866	−0.8858	0.2367
−0.5	3.50	0.6555	0.3847	0.0513	0.5948	0.848	−1.0942	−0.1556

[a] All energies in electron volts.

coordination number $N=4$ (or $N=6$). We shall now demonstrate that the ground-state structural and energetic theoretical parameters obtained herein are consistent with a variety of structural, thermodynamic, conductive, and magnetic relaxation data for dilute metal ammonia solutions.

The most important structural evidence for the cavity model in dilute metal ammonia solutions was based on the volume expansion data, namely, that the volume of, say, a sodium ammonia solution is greater than the volume of its constituents. This has been interpreted by Jortner[17] and others as indicating that the electron resides in a cavity of an effective radius of about $R_{\text{eff}}=3.2$ Å. Recent experimental results of Schindewolf[58] on the pressure dependence of equilibrium constants support this analysis of the experimental data. The theoretical significance of this effective radius $R_{\text{eff}}=3.2$ Å within the framework of our microscopic model is not immediately apparent. The value of R_{eff} can not be set equal to the value of R_0, nor can it be compared with the value of our void radius which was taken as $r_v=R_0-0.5$ Å [see Eq. (20)]. The difficulty arises since we have the first layer around the cavity with a density lower than the mean density of the bulk. The coordination number $N=4$, 6 is lower than the mean value in the medium because of the hydrogen–hydrogen repulsions (Sec. V). In this context it should be born in mind that for solid NH_3, $N=12$. Thus an apparent value expansion around the cavity is expected, resulting in a significant volume expansion.

Assuming a radius of the molecule in the first layer of 1.5 Å (from density measurements), the effective radius of our cavity is

$$R_{\text{eff}}^3=r_v^3+(r_v+3)^3-r_v^3-N(2.3)^3$$
$$=(r_v+3)^3-N(2.3)^3, \tag{40}$$

or the volume of the cavity plus the first layer minus the number of molecules found in this layer, assuming they occupied the same volume as in the bulk medium. Using $V_0=0.0$, for $N=4$ we obtain $R_{\text{eff}}=3.05$ Å, and for $N=6$, we obtain $R_{\text{eff}}=4.2$ Å. Both values are reasonable and again indicate the validity of our model. Larger effective cavity sizes for $V_0>0$ values are obtained when calculated using the above formula. The results are listed in Table VI.

The important qualitative conclusions arising from

TABLE V. Charge enclosed in the cavity for the most stable configuration.

N	C_s	C_p
$V_0=0.0$ eV		
4	0.210	0.020
6	0.336	0.053
8	0.458	0.119
$V_0=1.0$ eV		
4	0.283	0.028
6	0.446	0.089
8	0.575	0.218

the present discussion can be summarized as follows:

(a) In our microscopic model the electron cavity in liquid ammonia is characterized by a loosely packed first coordination layer. There is an appreciable amount of "empty" space in the first coordination layer relative to the bulk density. The electron charge density can "leak" through these vacant regions.

(b) The dipoles in the first layer are not rigidly oriented (at finite temperature of 200–500°K), as evident from the average values of the direction cosines listed in Tables III and IV.

There is currently a large bulk of experimental data which are consistent with the present model, although we must admit in all fairness that although this consistency is strongly indicative of the validity of our physical picture, it is by no means conclusive. We shall now list some of these experimental observations which are based on the interpretation of magnetic resonance and conductivity experiments:

(a) The analysis of nuclear magnetic relaxation data by Catterall[59] set the following limits on the coordination number:

$$3\leq N\leq 13;$$

thus our predicted data $N\approx 4$, 6 are consistent with this conclusion.

(b) In view of the large vacant space available for the leakage of the electron charge distribution within the first coordination layer, the electron can rather easily reform its cavity in another place. This conclusion is consistent with the fast nuclear relaxation times ($\tau\sim 10^{-11}$ sec) of the first solvation layer.[59]

(c) The short-lived structure around the electron cavity is also consistent with the relatively high value for the electron mobility ($\mu=10^{-2}$ cm^2/sec·V) in very dilute metal solutions (see Table I). This result cannot be quantitatively reconciled with a hydrodynamic motion of a rigid cavity, but is rather consistent with an "amoeba type" motion of the loosely packed structure of the first layer around the localized electron which is destroyed and rebuilt at a fast rate.

(d) The present model characterized by a loose structure around the localized excess electron is also in accord with the observation that the viscosity of metal ammonia solutions is lower than that of the pure solvent, in contrast to the behavior of ordering in ionic solutions.[60]

We shall now turn our attention to some thermochemical data for dilute metal ammonia solutions. The heat of solution ΔH of the electron is given to a good approximation by[17]

$$\Delta H=-E_t(1s) \qquad \text{at } R=R_0; \tag{41}$$

the experimental value of the heat of solution for e_{am}^- is from 1.7 to 1.0 eV,[17] the uncertainty in the estimate arising from our ignorance of the absolute heat of solution of the proton in liquid NH_3. In view of the qualitative discussion of Sec. II, it is reasonable to set V_0 close to zero, i.e., $-0.5\leq V_0\leq 0.5$ eV. The resulting heats of solution for the most energetically stable cavity configurations ($N=4$, 6) are close to the experimental heat of solution (see Tables III and IV). It should be born in mind that the present energetic data were obtained using a simple variational wavefunction for the calculation of the ground-state electronic energy E_{1s}. With more elaborate trial functions the energy E_{1s} and the resulting $E_t(1s)$ values are expected to be somewhat lower (but not more than a few percent).

Further information concerning the energy of the ground state can be obtained from the photoelectric threshold P for electron emission from metal ammonia solutions into the gas phase. The experimental value for the photoelectric threshold was found to be $P=+1.6$ eV. Theory predicts that

$$P\approx -E_{1s}(R_0). \tag{42}$$

Again for reasonable values of V_0 and for $N=4$, 6 the theoretical P values are located in the range 2.2–3.9 eV. It is not surprising that the theoretical P value exceeds the experimental result by a few tenths of an electron volt. It should be born in mind that this theoretical value [Eq. (22)] was computed at the equilibrium configuration of the electron cavity. Thermal motion of the cavity (with a fixed N value) will lead to populations of the ground-state vibrational states of the ground electronic state, and photoemission from these levels will occur at lower energies than from the equilibrium configuration ($R=R_0$). This effect is, of course, completely analogous to the broadening of the $1s\rightarrow 2p$ transition (see Sec. VIII) and will lead to a smearing of the photoelectric threshold towards lower energies. Thus the experimental P value provides a lower limit to the absolute value of the electronic energy at $R=R_0$. It is interesting to note that the combination of the values of ΔH and P provides us with a lower limit for the medium rear-

TABLE VI. Results for most stable molecular model cavities with various contributing factors for $T=300°K$.

V_0	R_0 (Å)	$E_t(R_0)$	E_{dd}	π	E_{H-H}	E_{1s}	$h\nu$	Estimated linewidth[a] Δ_a	$\langle\cos\theta\rangle$
$N=4$									
2.0	2.00	0.0103	0.1602	0.7792	0.0068	−1.0614	1.6507	0.20	0.864
1.5	1.85	−0.2929	0.1728	0.7920	0.0209	−1.3860	1.5191	0.16	0.849
1.0	1.80	−0.6301	0.1663	0.7861	0.0305	−1.7148	1.3755	0.15	0.830
0.5	1.75	−0.9933	0.1592	0.7781	0.0444	−2.0711	1.2529	0.14	0.808
0.0	1.72	−1.3770	0.1521	0.7687	0.0556	−2.4374	1.1404	0.15	0.784
−0.5	1.70	−1.7783	0.1358	0.7484	0.0646	−2.8178	1.0342	0.15	0.754
$N=6$									
2.0	2.50	−0.1459	0.3197	0.7155	0.0071	−1.3844	1.7845	0.30	0.868
1.5	2.40	−0.3645	0.3340	0.7233	0.0137	−1.6163	1.6351	0.24	0.861
1.0	2.30	−0.6132	0.3438	0.7212	0.0262	−1.8778	1.4789	0.20	0.850
0.5	2.25	−0.8945	0.3297	0.7228	0.0362	−2.1422	1.3024	0.18	0.832
0.0	2.25	−1.2078	0.3106	0.7044	0.0362	−2.4001	1.1115	0.17	0.808
−0.5	2.20	−1.5557	0.2693	0.6889	0.0502	−2.7161	0.9650	0.16	0.772

[a] Half-width estimated by the range of $h\nu$ included allowing for a variation of $E_t(1s)$ by kT, where k is Boltzmann's constant [see Eq. (56)].

rangement energy at the ground state as

$$E_M(1s)\geq P-\Delta H \tag{43}$$

as $E_M(1s)>0$ we expect that $P>\Delta H$. Taking $P=1.6$ eV and $\Delta H=1.0$ eV (which corresponds to the lower limit of the experimental estimate), we get $E_M(1s)>0.6$ eV, which is not inconsistent with our calculations (see Table III). This argument strongly supports the lower estimate $\Delta H\approx 1.0$ eV for the heat of solution of an electron in liquid ammonia.

TABLE VII. Effective and void radius at cavities obtained from present model.

		203°K		300°K	
N	V_0	r_v (Å)	R_{eff} (Å)	r_v (Å)	R_{eff} (Å)
4	2.00	1.50	3.46	1.50	3.25
	1.5	1.35	3.23	1.35	2.97
	1.0	1.30	3.14	1.30	2.86
	0.5	1.25	3.05	1.25	2.74
	0.0	1.22	2.98	1.22	2.68
	−0.5	1.20	2.95	1.20	2.62
6	2.0	2.00	3.74	2.00	3.45
	1.5	1.90	3.55	1.90	3.22
	1.0	1.85	3.46	1.80	2.99
	0.5	1.75	3.25	1.75	2.85
	0.0	1.75	3.25	1.75	2.85
	−0.5	1.70	3.14	1.70	2.71
8	2.0	2.50	4.10		
	1.5	2.45	4.02		
	1.0	2.40	3.92		
	0.5	2.35	3.83		
	0.0	2.35	3.83		
	−0.5	2.30	3.72		

Theoretical information intimately related to the photoelectric threshold involves the photoconductivity onset I, which simply is

$$I\approx -E_{1s}(R_0)+V_0, \tag{44}$$

where again the broadening due to thermal motion was neglected. For $N=4$ we expect I to range from 2.8 eV for $V_0=1.0$ eV to 2.4 eV for $V_0=-0.5$ eV. The values for $N=6$ are not very different.

Some further information concerning the ground state of the solvated electron in ammonia can be obtained from the frequency of the totally symmetric vibration in the ground state, which is given by

$$\nu_s=(1/2\pi)(K/\mu)^{1/2}, \tag{45}$$

where the force constant K is $\frac{1}{2}(\partial^2 E_t/\partial R^2)_{R=R_0}$, while the effective mass is $\mu=Nm_{NH_3}$, m_{NH_3} being the mass of the ammonia molecule. The values of ν_s calculated from the ground-state configuration diagram are assembled in Table VII. This vibrational mode may be monitored by Raman scattering from metal ammonia solutions.

To conclude this discussion, we have presented in Table VIII a comparison between the predictions of our model and the available experimental data. We have included also some pertinent information concerning optical properties which we shall now proceed to discuss.

VIII. OPTICAL PROPERTIES

The configuration diagrams obtained for the ground $(1s)$ and for the first excited $(2p)$ state enable us to gain some theoretical insight into the nature of the

TABLE VIII. Properties of the totally symmetric vibration at 203°K.

	N	V_0	Second derivative at minimum (eV/Å²)	$\bar{\nu}$ for symmetric vibration (cm^{-1})
Ground state	4	2.0	0.316	25.0
		1.5	0.716	37.7
		1.0	0.978	44.1
		0.5	1.376	52.3
		0.0	1.96	62.4
		−0.5	1.94	62.0
	6	1.0	0.623	28.7
		0.5	1.007	36.5
		0.0	0.974	35.9
		−0.5	1.268	41.0
	8	0.5	1.018	31.8
		0.0	0.995	31.4
		−0.5	1.245	35.1
Excited state	4	0.5	0.140	16.6
		0.0	0.199	19.9
		−0.5	0.237	21.7

optical excitation processes which are responsible for the broad structureless absorption band of dilute metal ammonia solutions and of the solvated electron in other polar solvents. Such configuration diagram curves are also of obvious interest in ascertaining the energetic stability of excited states and the nature of radiative and nonradiative decay of excited electronic states. Such configuration diagrams have been extensively used in solid state theory to account for the properties of impurity states in solids. Obviously a generalized configuration diagram should specify the energy of the system as a function of (a large number of) nuclear displacements. The choice of a single configurational coordinate for this purpose is by no means obvious, and a general theory of multiphonon processes in solids was provided to justify the use of such a single (temperature-dependent) configurational coordinate. Even this general treatment still suffers from the application of the harmonic approximation for nuclear displacements. In what follows we shall adopt a simpler but hopefully a realistic approach and consider the single totally symmetric breathing mode of the electron cavity (specified by the coordinate R) to specify the dependence of the total energy of a given electronic state on the nuclear configuration. This approximation immediately implies that:

(a) The dependence of the electronic energy on other nontotally symmetric vibrational modes is weak.

(b) The triply degenerate $2p$ state is not split by the totally symmetric vibration.

If nontotally symmetric modes strongly couple electronic and nuclear motions, a Jahn–Teller splitting of the excited state would be manifested in the optical spectrum.

Using the rather drastic assumption (common to many semiquantitative treatments in solid state theory) concerning the dominant role of the totally symmetric vibration, we can then utilize the configuration diagrams displayed in Figs. 18–21 for the study of the optical properties of the solvated electron in liquid ammonia. A cursory examination of these configuration diagrams leads to the following general conclusion:

(a) A fair approximation for the energy corresponding to the maximum of the absorption band is given by the vertical energy gap between the $1s$ and $2p$ curves calculated at $R=R_0$,

$$h\nu = E_{2p}(R_0) - E_{1s}(R_0). \tag{46}$$

In Table IX we list the results obtained from our model. For V_0 close to zero and $N=4$, 6 (which are the proper values to account for the configurational stability of the ground state), the agreement between theory and the experimental value for the maximum of the absorption band is reasonable, although by no means quantitative.

(b) The integrated oscillator strength calculated from the transition moment (Table IX) is lower than the experimental values. This is by no means a sensitive criterion as Jortner's polaron model yields $f=0.582$.

(c) The potential surfaces are temperature dependent. This effect arises mainly from the enhanced thermal motion of the dipoles in the first solvation layer with increasing temperature, with the temperature dependence of β providing another source of temperature variation. The first effect provides, in fact, a crude description of the temperature dependence of the *local* (microscopic) dielectric constant. This feature of temperature-dependent configuration diagrams is unique for the solvated electron, which is localized due to a self-trapping mechanism. To obtain a rough idea of the magnitude of this effect, we notice that from Tables VIII and IX, $dh\nu/dT \approx -4\ cm^{-1}/deg$. This value *cannot* be directly related to the temperature shift of the band maximum in the absorption spectrum because the ground-state configuration curve is far from being harmonic and thermal expansion effects must be introduced. With the availability of proper configuration diagrams these effects can be properly handled.

(d) The ground-state configuration diagram $E_t(R)$ shows a marked deviation from a parabolic curve. Thus at finite temperatures the mean radius of the cavity will be larger than R_0 (the minimum value). Thus the marked anharmonicity of the ground-state configuration diagram leads to thermal expansion of the cavity. This effect of thermal expansion previ-

TABLE IX. Summary of properties of model for $N=4$.

	Experimental values (See Table I)	$V_0=+0.5$		$V_0=0.0$		$V_0=-0.5$	
		203°K	300°K	203°K	300°K	203°K	300°K
Transition energy $h\nu$ (eV)		1.303	1.253	1.192	1.140	1.087	1.034
Maximum of line shape, $h\nu_{max}$	0.80	1.302	1.246	1.189	1.137	1.080	1.028
Bandwidth (eV)		0.107	0.122	0.105	0.124	0.106	0.123
Oscillator strength	0.77	0.48	0.48	0.49	0.50	0.50	0.51
Temperature coefficient of $h\nu_{max}$ (cm^{-1}/°K)	-12[a]	-4.7		-4.3		-4.3	
Equilibrium radius of cavity, R (Å)		1.75	1.75	1.72	1.72	1.75	1.70
Effective radius of cavity, R_{eff} (Å)	3.2	3.1	2.7	3.0	2.7	3.1	2.6
Heat of solution ΔH (eV)	1.7±0.5	1.05	0.99	1.43	1.38	1.83	1.78
Photoelectric threshold, P (eV)	1.6	2.18	2.07	2.56	2.45	2.93	2.82
Photoconductivity threshold, I (eV)		2.68	2.57	2.56	2.45	2.43	2.32
Average radius of 1s electron (Å)		3.08	3.16	3.24	3.33	3.45	3.56

[a] R. K. Quinn and J. J. Lagowski, J. Phys. Chem. 73, 2326 (1969). A value of -19 cm^{-1}/°K has been reported recently by Tuttle and Golden (private communications).

ously invoked to account qualitatively for the temperature dependence of the energy of the maximum of the absorption band, $h\nu_{max}$, is of crucial importance in determining both $dh\nu_{max}/dT$ and the shape of the intensity distribution in the absorption band.

Obviously equating $h\nu$ to $h\nu_{max}$ is strictly legitimate only for low temperatures $kT \ll h\nu$ [where ν was defined by Eq. (45)]. At high temperatures the deviation of $h\nu$ from $h\nu_{max}$ is of considerable importance for the understanding of the line shape problem.

Our treatment of intensity distribution in absorption rests on the two following assumptions:

(a) At high temperatures ($kT \gg h\nu$) we can apply classical statistics for the population of the ground state. This approximation is wholly justified in the temperature region 200–300°K.

(b) The semiclassical Condon approximation is invoked, whereupon the electronic transition moment is independent of the nuclear configuration. This is satisfied quite well over the ranges of R considered.

Adopting these assumptions the line shape is determined by the thermal population of the ground state and by the dependence of the vertical transition energy on R. Let the displacement of the collective coordinate R from equilibrium be denoted by

$$X=R-R_0=r_v-(r_v)_0, \tag{47}$$

and let the total ground-state energy at $R=R_0$ be denoted by $E_t^0(1s)$. Then the ground-state configuration diagram can be written in the form

$$A(X)=E_t(1s)-E_t^0(1s). \tag{48}$$

The (unnormalized) intensity distribution function $F(E)$ for optical excitation at the energy E can be displayed in the form

$$F(E)=\exp[-A(X)/kT]\,|\,dX/dE\,|, \tag{49}$$

where the factor $|\,dX/dE\,|$ is the Jacobian which transforms from the configuration space to the energy space. To evaluate this term we set

$$E_t(2p)=B(X), \tag{50}$$

$$E(X)=B(X)-A(X), \tag{51}$$

so that

$$dX/dE=[B'(X)-A'(x)]^{-1}\equiv C(X), \tag{52}$$

where the primes denote derivatives with respect to X. Thus the intensity distribution in absorption is given by

$$F[E(X)]=\exp[-A(X)/kT]\,|\,C(X)\,|. \tag{53}$$

Before proceeding to detailed calculations for the solvated electron, the following general features of these results have to be noticed:

(a) *The half-linewidth of the absorption band.* Let X_1 and X_2 correspond to the points where $F(X_1)=F(X_2)=kT\ln 2$; then the half-bandwidth Δ is given in the form

$$\Delta=|\,E(X_1)-E(X_2)\,|. \tag{54}$$

To obtain an estimate of the half-linewidth we sometimes used a procedure, namely, we simply considered the points where $A(X_3)=A(X_4)=kT$ and evaluated

$$\Delta_a=|\,E(X_3)-E(X_4)\,|. \tag{55}$$

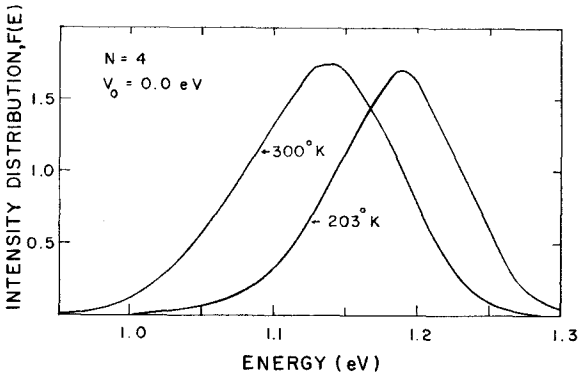

FIG. 22. Calculated line shape for the $1s \rightarrow 2p$ transition based on the molecular calculations with $N=4$ and $V_0=0.0$ eV.

This is the number listed in Tables II, IV, and IX. All other tables list the exact form, Eq. (54).

(b) *The maximum of the absorption band.* The energy $h\nu_{\max}$ corresponding to the maximum of the absorption band can be obtained from Eq. (53) by setting $dF(E)/dE=0$, and as $dX/dE \neq 0$ we have

$$(dF/dX)_{X_M}=0. \tag{56}$$

The value of $X=X_M$ obtained from Eq. (56) corresponds to the band maximum

$$h\nu_{\max}=E(X_M). \tag{57}$$

Now Eqs. (53) and (56) lead to the following relation for X_M:

$$[dA(X)/dX]|_{X=X_M}=kT[d \ln |C(X)|/dX]|_{X=X_M}. \tag{58}$$

It is important to notice at this point that in general X_M and $h\nu_{\max}$ are temperature dependent. Obviously $X_M=0$ only for the limit of low temperatures $T \rightarrow 0$ [in this case our equations have to be modified by introducing a quantum temperature $T=(h\nu/2k)\times \coth(h\nu/2kT)$]. The relation $h\nu \approx h\nu_{\max}$ is adequate only for energy level calculations; however, when the temperature dependence of the absorption band is considered, a complete calculation based on the relations presented herein is required.

(c) *Asymmetry of the absorption band.* In general the distribution represented by Eq. (8) is not symmetric around $E=h\nu_{\max}$. The asymmetry may arise from two factors: $A(X)$ in the exponential may include odd powers of the energy or the excitation energy includes a second-order term $O(X^2)$ and terms higher than linear in the reduced displacement so that $|C(X)|$ contains an odd function of the energy. Such contributions will arise in a general case, in particular when anharmonicity effects are included.

In Appendix A we present simple detailed models of how such features could appear in an absorption spectrum. From those results one can see the effects of various factors on the shape of the potential curves most markedly.

As regards our calculations, we can obtain the functions $A(X)$ and $B(X)$ from Figs. 18–21 and the value of dX/dE from the data in Figs. 15–17. This is all one needs to obtain the intensity distribution. In view of the unique temperature dependence of the configuration diagrams such calculations have to be performed separately for each temperature. In Figs. 22 and 23 we present the intensity distributions for the cases $N=4$ and $V_0=0.0$ and 0.5 eV, while a summary of the optical properties is given in Table X.

From these results we conclude that

(a) The major contribution to $d(h\nu)/dT$, namely, the change in the force constants with temperature, is due mainly to the effect of temperature on the orientation of the dipoles in the first layer.

(b) The values of $h\nu$ and $h\nu_{\max}$ are quite close, indicating that the harmonic approximation is reasonably accurate at these temperatures.

(c) The line shapes are definitely asymmetric but to the low-energy side, contrary to the experimental observations.

(d) The linewidths calculated from the present model are quite large (0.1–0.13 eV) but still a factor of 3 or 4 below the experimental values.

It should be born in mind that the present model is based on a one-dimensional configuration diagram and other vibrational modes of the cavity may conceivably contribute to the line broadening. It should be also recalled that we have assigned the line broadening to the thermal motion of a single structure of solvent molecules whereupon the cavity is characterized by a constant coordination number $N=4$. We have already stated that various types of cavities (characterized by different N values, presumably in the region of $N=4$, 6) may coexist in the solution as their ground-state energies are calculated to be within 0.1 eV. Thermal equilibrium between different structures each characterized by a coordination number N with minimum ground-state energy $E_t^N(R)$, a transi-

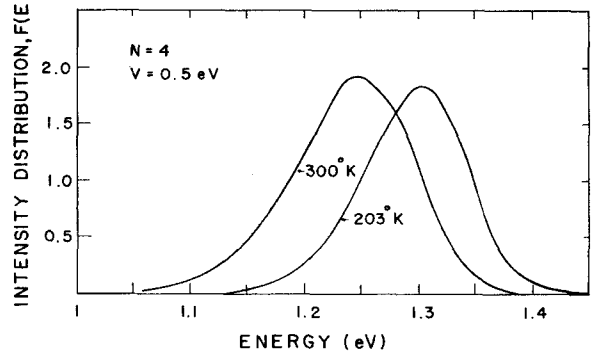

FIG. 23. Calculated line shape for the $1s \rightarrow 2p$ transition based on the molecular calculations with $N=4$ and $V_0=0.5$ eV.

TABLE X. Optical properties of electrons in ammonia.

		203°K			300°K			
V_0	R_0	Transition energy $h\nu$ (eV)	Estimated bandwidth[a] Δ_a	Oscillator strength	Transition energy $h\nu$ (eV)	Estimated bandwidth[a] Δ_a	Oscillator strength	$d(h\nu)/dT$ (cm^{-1}/°K)
$N=4$								
1.0	1.80	1.4223	0.13	0.466	1.3755	0.15	0.468	−3.89
0.5	1.75	1.3028	0.12	0.479	1.2529	0.14	0.483	−4.15
0.0	1.72	1.1924	0.12	0.491	1.1404	0.15	0.497	−4.32
−0.5	1.70	1.0872	0.13	0.503	1.0342	0.15	0.509	−4.36
$N=6$								
1.0	2.35	1.5015	0.21	0.477	1.4789	0.20	0.477	−1.88
0.5	2.25	1.3586	0.16	0.484	1.3024	0.18	0.486	−4.67
0.0	2.25	1.1728	0.15	0.495	1.1115	0.17	0.499	−5.10
−0.5	2.20	1.0319	0.14	0.507	0.9650	0.16	0.514	−5.56
$N=8$								
1.0	2.90	1.4637	0.18	0.477				
0.5	2.85	1.3021	0.16	0.488				
0.0	2.85	1.1035	0.14	0.498				
−0.5	2.80	0.9338	0.14	0.410				

[a] Estimated according to Eq. (57) in paper. For accurate values see Table VIII.

tion energy $E^N(R)$, and an individual line shape $F_N[E^N(R)]$ given by Eq. (53), and a (mean) oscillator strength f_N will lead to an absorption band of the form

$$F(E)=\sum_N f_N F_N \exp[-E_t^N(R)/kT] \times \{\sum_N \exp[-E_t^N(R)/kT]\}^{-1}. \quad (59)$$

Our theoretical results seem to discard this interpretation on the basis of the following arguments: (1) The spread in excitation energies between $N=4$ and $N=6$ cavities calculated on the basis of our model is ~0.1 eV, which is too small to account for the discrepancy between theory and experiment. (2) The most stable configuration ($N=4$) is characterized by the highest excitation energy. Hence even if somewhat less stable configurations contribute a few percent to the generalized line shape (59), these will have lower excitation energies (see Table II) and thus will lead to broadening on the low-energy side of the band in contrast to experiment.

An alternative interpretation of the additional source of line broadening invokes the old idea concerning the role of higher ($n\geq 3$) excited states, which on the basis of the intensity calculation (Tables VII and IX) should carry an oscillator strength of the order of ~0.4–0.5[61] (the oscillator strength to the conduction band is expected to be low!). These states will be again broadened and will contribute to the observed asymmetry and linewidth.

(e) The present model based on the thermal population of the ground-state levels of a single structure (constant N) predicts that the half-linewidth should reveal a temperature dependence roughly proportional to $T^{1/2}$. This behavior is common to all temperature-dependent phonon broadening processes at high temperatures. Thus the half-linewidth should increase by about 20% in the temperature region 200–300°K. This is in accord with our observations in Table VIII. The old results of Blades and Hodgins[62] seem to be consistent with this elementary prediction. However, new data of Quinn and Lagowski[63] (and Tuttle and Golden[64]) seem to indicate that the linewith in extremely dilute metal ammonia solutions is practically temperature independent. The Quinn and Lagowski value is based on a wavelength plot and thus if converted to an energy scale could show a slight temperature dependence. If these new data are confirmed, the answer must either lie in a compound line shape such as Eq. (60) or more likely in the existence of higher excited states since then the major factor determining line shape would be the separation of the various transition energies and not the broadening of any one transition.

(f) Finally there is another class of measurements, namely, the effect of pressure on the optical spectra as measured by Schindewolf and co-workers for 200 to 1100 atm.[58] It was observed experimentally that the spectra move to higher energies and broaden with increased pressure. The trend in the band maximum is obviously explained by our model. As the pressure increases, the cavity size decreases and the first figures of this paper (or even the very crude polaron or

TABLE XI. The hydrated electron at 298°K.

V_0	R_0	A	E_{1s}	D	E_{2p}	$E_t(s)$	$\langle\cos\theta\rangle$	$h\nu$
$N=4$								
2.0	1.35	0.6617	−1.7208	0.5186	0.4081	−0.05877	0.9049	2.1289
1.5	1.15	0.6589	−2.1879	0.5122	−0.0808	−0.44098	0.8934	2.1071
1.0	0.50	0.7698	−3.2340	0.5185	−1.5844	−0.92156	0.7620	2.6446
0.5	0.50	0.7634	−3.7078	0.5184	−1.0891	−1.41388	0.7571	2.6187
0.0	0.50	0.7569	−4.1820	0.5182	−1.5888	−1.90677	0.7520	2.5932
−0.5	0.50	0.7507	−4.6567	0.5181	−2.0886	−2.39979	0.7470	2.5682
$N=6$								
2.0	2.00	0.6745	−2.1279	0.6202	0.2139	−0.05314	0.9186	2.3418
1.5	1.90	0.6568	−2.4130	0.5766	−0.1997	−0.30613	0.9154	2.2133
1.0	1.80	0.6385	−2.7293	0.5459	−0.6406	−0.58528	0.9111	2.0887
0.5	1.75	0.6127	−3.0344	0.5752	−1.1004	−0.89308	0.9045	1.9339
0.0	1.65	0.5961	−3.4125	0.5110	−1.5731	−1.22812	0.8978	1.8395
−0.5	1.60	0.5728	−3.7700	0.5002	−2.0517	−1.59047	0.8888	1.7183

particle in a box model) predict a trend to higher transition energies. Quantitative predictions are complicated by the possibility of having several sized cavities since the effect of pressure is different on each. In addition the actual volume involved in the pressure–volume work is somewhat complicated by the fact that the density in the first layer around the cavity differs from that of the bulk media. A cursory study of the configuration diagrams shows that the value of R_0 cannot decrease too much under pressure since the molecule–molecule repulsion rapidly becomes very large. This is in agreement with the experimental results which show significant but small changes in the position of the band maximum. This problem deserves a further study.

We conclude this discussion with some speculations concerning the energetic stability of excited electronic states: (1) The $2p$ localized excited state is stable relative to the quasifree electron state (see Figs. 19–21, for example). This state is located about 0.3–0.7 eV below V_0, so thermal excitation to the conduction band will be negligible.[51] (2) The photoconductivity threshold corresponding to direct excitation to the conduction band is ~2.4–2.7 eV (see Sec. VII). There may be autoionizing states overlapping the ionization continuum. However, such states will be appreciably broadened. As the onset for bound–free transition of the electron in ammonia is expected to be located in the region 4000–5000 Å, it is surprising that photoconductivity was not yet reported in this region. Experimental difficulties due to the use of weak light sources may be responsible for this failure as the relaxation process which involves electron solvation is very fast (of the order of the dielectric relaxation of the pure solvent). The utilization of laser sources (i.e., first and second harmonic of ruby and nyodinium solid state lasers, at 10 000 Å, 6970 Å, 5300 Å, and 3475 Å) will be of considerable interest. Laser photolysis experiments of extremely dilute metal ammonia solutions (where the reactivity of the cation with the excited state of the solvated electron is negligible) will be of considerable interest to establish the intrinsic photoionization threshold. (3) As the $2p$ excited state is bound, it may decay either radiatively or nonradiatively to the ground state.[51] The radiative decay process is expected to exhibit a large (~0.3 eV) Stokes shift due to the displacement of the minimum of the excited state (see Fig. 20, for example). Nonradiative decay between the excited state and the ground state will now be briefly considered. Provided that the configuration diagrams cross in the vicinity of the vertical excitation energy from the ground state, the excited configuration will decay nonradiatively.

If the crossing point is higher, thermally activated nonradiative decay will take place from the minimum of the excited state. Our results indicate that such crossing between the $2p$ and $1s$ states is not feasible. On the other hand, one should bear in mind that the optically forbidden $2s$ state may be located close to the $2p$ state. This situation may result in an efficient nonradiative decay which is due to the crossing between the potential curves of the $2p$ and the $2s$ configurations, followed by a nonradiative decay of the $2s$ state to the ground state. Further calculations are needed on these points and on the "relaxed" $2p$ states, i.e., states calculated in which the dipoles are allowed to reorient in response to the actual $2p$ electronic distribution [compare this to Eq. (25) in which the potential is determined by the $1s$ electronic distribution].

IX. OTHER SOLVENTS

The discussion in the previous sections has centered around electrons in ammonia. However, electrons can exist for various lengths of time in other polar sol-

TABLE XII. Charge densities of the hydrated electron.

V_0	R_0	C_s	C_p
$N=4$			
2.0	1.35	0.266	0.014
1.5	1.15	0.195	0.007
1.0	0.50	0.043	0.000
0.5	0.50	0.042	0.000
0.0	0.50	0.041	0.000
−0.5	0.50	0.041	0.000
$N=5$			
2.0	2.00	0.506	0.106
1.5	1.90	0.455	0.071
1.0	1.80	0.404	0.050
0.5	1.75	0.362	0.039
0.0	1.65	0.314	0.029
−0.5	1.60	0.278	0.024

vents. The ideas presented above apply to the other systems as well although in some cases certain terms dominate others. This is particularly true in regard to medium rearrangement contributions. As presented, our examples have assumed that the solvent was small and easily oriented. Similar approaches may hold in regard to parts of large molecules and as such could explain the observation of localized electrons in frozen sucrose solutions.[65] In the main, however, we must consider small molecules.

As an example we are well aware that one can have a localized electron species in water.[66,67] The observed spectra are similar but the transition is at slightly higher energy in water than ammonia. In studies of the pressure dependence of the reaction of solvated electrons with water, Schindewolf and coworkers[58] found that the hydrated electron has essentially no volume in contrast to the ammonia case where it has an effective radius of about 3.2 Å or a volume from Schindewolf's arguments of probably 75±12 ml/mole at −33°C.

In the case of water we expect our parameter, V_0, the energy of a quasifree electron, to be less than that of ammonia due to the larger dipole moment and the more open structure of water at low temperatures. For convenience we can select it as equal to zero.

The other major difference between ammonia and water which we must introduce explicitly is the geometry of the molecule. In particular, the orientation of the hydrogens is not the same in the two cases. In the case of ammonia with its three hydrogens the molecule can only reduce its contacts with its neighbors around the cavity a small amount by rotating along the dipolar axis. If it rotates too far, other hydrogens will begin to get close together. With water the molecule can reduce hydrogen–hydrogen repulsions significantly by rotating. For this reason, it is a better approximation to neglect the term E_{HH}, Eq. (31), entirely. As to the size of the water molecule we choose $\tilde{a}$, the hard core, as 1 Å and r_s, the radius of the solvent molecule, as 1.5 Å. These are reasonable parameters and are identical to those used for ammonia. The calculations are quite insensitive to these numbers for their major role is to define the radius at which the continuum begins. In our calculations all solvent-molecule–hydrogen repulsions are neglected and thus the smallest cavity one can obtain corresponds to $R=0.5$ Å or a zero void radius. In Tables XI and XII we present some of the results of our calculations on the hydrated electron using the model of this paper with the appropriate dipole moment, polarizability, and surface tension, but neglecting all water–water repulsions. For $V_0=0.0$ (and several other values) with $N=4$, the most stable configuration, we observe that the optimum cavity size has a zero void volume. Because of this we can produce no configuration diagrams or line shapes. Including the repulsion of hydrogens from water molecules on opposite sides of the cavity would yield a curve with a potential minimum very close to the one observed but whose configuration diagram could be determined. These calculations were not done because the basic factors are already demonstrated by the present calculations. The results indicate the hydrated electron should be quite localized (note, however, the low values for charge enclosed) and have a much higher transition energy than the electron in ammonia. These factors are in qualitative (in some cases even quantitative) accord with all known data on the hydrated electron.

Our results are also consistent with data in other solvent systems. Consider the alcohols, from our arguments the properties should be strongly dependent on the shape of the molecule, especially that part of the molecule which makes up the cavity walls. Thus it is not surprising that tertiary butanol has a transition energy similar to 2-propanol,[67,68] but very different from 1-butanol. Any attempt to relate these by their dielectric constants fails.[68] Because of the increased repulsion between solvent molecules, electrons in 2-propanol have a much smaller transition energy than electrons in 1-propanol.[68] Considering the differences in the liquid ranges and other variations, ethanol, methanol, and 1-butanol lead to remarkably similar transition energies for the solvated electrons.[68] 1-Propanol is also similar but slightly out of line with this very qualitative analysis.

Data on amines would be most interesting, but most of this data is for concentrations of alkali metal in which there appears to be significant electron spin pairing and probably other species present. The absorption in ethylene diamine as studied by pulse radiolysis suggests that the solvated electron has an absorption maximum above 10 000 Å[69] and possibly as high as 12 800 Å (0.6 eV), a value obtained for one peak in dilute alkali metal amine solutions.[70] The

geometry of this molecule suggests strong repulsion between solvent molecules in the first layer and thus a low transition energy, in rough accord with the observations. The complication with the amines is that the dipole moment has both its direction and magnitude altered by substitutions on the nitrogen, and so their orientation on the boundary of the cavity is not simple to interpret. What we clearly need are more studies on the smaller amines where it may be easier to make simple qualitative interpretations.

X. DISCUSSION

In this paper we have attempted to present a microscopic model for excess electron states in polar solvents with a special emphasis on the physical properties of dilute metal ammonia solutions. The purpose of the exercise is not to reproduce experimental results, which are currently determined in a much more reliable manner in the laboratory, but rather to try to elucidate the pertinent physical factors which determine the stability of a localized ground state, the physical properties of this state and the nature of excited electronic states of excess electrons in polar solvents.

A detailed calculation of the electronic energy and of the medium rearrangement energy has been provided. Although these calculations are admittedly approximated and some of their features will be soon improved upon, we believe that the present results are useful to demonstrate the major theoretical ingredients which have to be introduced in such a study. In the calculation of the electronic energy we have considered the electronic kinetic energy and the short-range attractive interactions on the basis of a molecular model while short-range repulsions and long-range polarization effects were introduced by a "coarse grain" averaging method. The medium rearrangement energy was handled by the introduction of a molecular model for the first solvation layer, using a continuum approximation beyond it. The present treatment was rather successful in predicting and interpreting semiquantitatively a variety of structural, thermodynamic, and optical properties of metal ammonia solutions, and of the hydrated electron such as the size of the electron cavity, the heat of solution, optical excitation energies, line shapes in the optical spectrum, photoelectric thresholds, and photoionization onsets. The number of adjustable parameters entering into the theory is minimal. Apart from the unknown value of the short-range repulsion term V_0 (which is not expected to be far from $V_0=0$), the present treatment can provide a reasonable estimate of the ground-state configuration of the solvated electron in simple polar solvents.

The major general conclusions arising from the present study can be summarized as follows:

(a) In order to understand the properties of the solvated electron in polar solvents, one cannot get away with the calculation of only the electronic energy. The medium rearrangement energy plays a crucial role in determining the ground-state configuration and the physical properties of the solvated electron. Inclusion of the medium rearrangement energy is also crucial for the understanding of the different properties of the solvated electron in different solvents. It is hoped that people interested in the properties of the solvated electron now will stop performing calculations for an arbitrary cavity size which is chosen to fit some experimental data.

(b) The major physical reasons for the stability of a localized ground state of an excess electron in polar solvent can be now traced to the following physical factors:

(1) V_0 is not far from $V_0=0$ and the general stability conditions are thus satisfied, Eqs. (4) and (39). For a hypothetical solvent characterized by large negative V_0 (say $V_0\approx-2$–3 eV), the quasifree electron state would have been energetically favored.

(2) The potential acting on the electron is characterized by a large negative potential within the cavity, which leads to large negative values of the electronic energy. This feature is not unique to the present microscopic model and can be considered as almost model independent since it also appears in the polaron model and can even be incorporated in the primitive electron in a box model.

(3) The present treatment of the electronic energy and of the total energy of the solvated electron involves a major extension of the old Landau self-trapping model, whereupon the role of short attractive interactions is now properly introduced.

(4) The present approach based on the configurational diagrams for the ground and excited states of the solvated electron has many features in common with the conventional picture of F center and impurity centers in solids. The major difference between electron trapping in a crystal anion vacancy and the solvated electron is that in the latter case the electron reorganizes the solvent ("digging its hole" in the old terminology) and thus the configuration diagrams have to be determined in a self-consistent manner. This is obviously also the reason that the configuration diagrams are temperature dependent.

(5) The interpretation optical spectrum of the solvated electron should not be limited to the energy of the band maximum, but rather the whole line shape should be considered. The broadening arising from thermal motion is responsible for a major portion of the linewidth of the bound-bond $1s\rightarrow 2p$ transition. Similar considerations should be applied for an interpretation of the energy dependence of an external photoemission cross sections and the intrinsic photoionization data, if these will become available.

(6) A unique feature of the extended self-trapping model which is strongly dependent on the physical

picture of Landau involves the Coulombic form of the long-range attractive potential due to the permanent dipoles. This potential can sustain an infinite number of excited levels converging to the photoionization threshold which should be observed at about 2.5 eV in NH_3. Other models such as an electron in a finite box are unrealistic in this respect as they can sustain only a finite number of excited states. That is the reason why photoconductivity (or alternatively, laser flash photolysis) data are of such intrinsic importance for the understanding of the excited states of these systems and of their time-dependent behavior.

There are currently several interesting problems which deserve further theoretical study to gain a deeper insight into the nature of electrons in polar solvents:

(a) Theoretical calculation of V_0 in polar solvents.

(b) More elaborate calculations of the electronic energy of the ground and higher excited states using better trial functions. This task was recently carried out by Copeland and Kestner.[71]

(c) The location, intensity and width of higher excited states is of considerable interest for the understanding of the asymmetric broadening of the absorption band of the solvated electron. The nature of these states depends critically on the exact definition of V_0.[51]

(d) The nature of electronic nuclear coupling in the triply excited $2p$ state is of considerable interest both in the context of the general Jahn–Teller effect and in relation to the problem of the solvated electron. A general formulation of the line shape problem including nontotally symmetric distortions will be reported by one of us (J. J.).

(e) Relaxation phenomena of these excited electronic states are of considerable interest; these were recently handled by one of us (J. J.) using a general theory of nonradiative processes.[72] An additional complication in this case is that the dipole moments can also relax under the excited-state electronic distribution.

(f) A closely related problem involves the properties of the positron and of the positronium atom in polar solvents which can be studied by positronium annihilation methods.[73–75] It is amusing to notice that as the positron does not suffer from the exclusion principle, the energy of a quasifree positron in a polar solvent such as an ammonia is expected to consist just of the contribution of long-range polarization interactions. Thus adopting the notation of Sec. II for positron, $T=0$ and $V_0=U_p\approx-3$ eV, and this particle is not expected to be localized. On the other hand, for the neutral positronium atom the long-range polarization interaction are switched off, whereupon $U_p=0$ and $V_0=T=+3$ eV. Hence the positronium is expected to be localized in a polar solvent due to short-range repulsion. The effective potential will be $V(r)=0$ for $r<R$ and $V(r)=V_0$ for $r>R$. This picture is completely analogous to that applied for positronium bubbles in nonpolar liquids. This problem deserves a more serious further study, both theoretically and experimentally.[76]

APPENDIX A: EFFECT OF THE FORM OF THE POTENTIAL ENERGY SURFACE ON THE ABSORPTION SPECTRA LINE SHAPE

In Sec. VIII we mentioned qualitatively how various features of the potential curves could affect the line shape of the absorption spectra. In this Appendix we present model systems which represent the temperature dependence of $h\nu_{max}$ and an asymmetric line shape.

The model we shall choose concerns the optical line shape due to the transition between the two harmonic one-dimensional surfaces which are characterized by different temperature-independent force constants. The ground state is

$$A(x)=\tfrac{1}{2}Kx^2 \tag{A1}$$

while the excited state is represented by

$$B(x)=\tfrac{1}{2}K'(x+x_0)^2+\bar{\alpha}, \tag{A2}$$

so the transition energy is

$$\begin{aligned}E(x)&=B(x)-A(x)\\&=h\nu+K'x_0x+\tfrac{1}{2}(K'-K)x^2,\end{aligned} \tag{A3}$$

with a vertical excitation energy at $x=0$ of

$$h\nu=\bar{\alpha}+\tfrac{1}{2}K'x_0^2. \tag{A4}$$

Making use of Eq. (58), we obtain the following relation for the coordinate value corresponding to the maximum in the absorption line, x_M:

$$\frac{Kx_M}{kT}=-\frac{|K-K'|}{|K'x_0+(K'-K)x_M|}. \tag{A5}$$

It is safe to assume that $|K'x_0|\gg|(K'-K)x_M|$, whereupon

$$x_M=-|K-K'|kT/K|K'x_0|. \tag{A6}$$

Making use of Eqs. (57) and (A3), the maximum energy of the absorption band can be displayed as a power series in kT, the leading terms being

$$h\nu_{max}=h\nu+(|K-K'|/K)kT+\cdots. \tag{A7}$$

The temperature coefficient of the absorption band is

$$dh\nu_{max}/dT=+(|K-K'|/K)k. \tag{A8}$$

This is always positive, an important point regarding the interpretation of spectral data. Although the calculations in this paper suggest that $K'<K$, the sign is independent of such assumptions provided that the conditions leading to Eq. (A6) are met. The results

are also contrary to the actual calculations. In addition, if $K' \ll K$ the maximum value for the derivative is only about $+0.7$ cm^{-1}/°K.

We next consider the line shape for this model system. Making use of Eq. (A3), we can write the displacement x as

$$x = \frac{(K'x_0)[1+2(K'-K)\Delta E/(K'x_0)^2]^{1/2} - K'x_0}{K'-K}$$
$$\approx \Delta E/K'x_0 + \tfrac{1}{2}(K-K')\Delta E^2/(K'x_0)^3 + \cdots, \quad \text{(A9)}$$

where $\Delta E = E - h\nu$ and we have assumed $(K'-K) \ll K'$ as well as $2\Delta E/K'x_0^2 < 1$. The line shape following Eq. (53) is

$$F(\Delta E) = \frac{\exp[-(K/2kT)(a^2\Delta E^2 + 2ab\Delta E^3 + b^2\Delta E^4 + \cdots)]}{|(K'-K)(a\Delta E + b\Delta E^2) + K'x_0|}, \quad \text{(A10)}$$

in which $a = 1/K'x_0$ and $b = (K-K')/[2(K'x_0)^3]$.

Provided that $x_0 < 0$ (i.e., the equilibrium point of the excited state is located at a positive value of x, and $K' < K$ (the typical situation), we find that both a and b are negative. Thus the term $2ab\Delta E^3$ in the exponent will lead to an asymmetry for $\Delta E < 0$, e.g., at lower energies. However, the denominator $|dx/dE|$ of Eqs. (58) or (A10) leads to an asymmetric line, asymmetric toward higher energies. This dominates for small ΔE as demonstrated by the shift in the maximum, Eq. (A7). Finally, we should notice that when $K = K'$, $b = 0$ and Eq. (A10) reduces to a Gaussian line shape function and $h\nu_{\max} = \Delta E$ for all temperatures as expected from Eq. (58).

From these results for the simple model system we conclude that:

(a) In the high-temperature limit the line shape is Gaussian and $h\nu_{\max}$ is temperature independent only for transitions between two displaced harmonic surfaces which are characterized by the same force constants. This result is well known from the work of Lax[77] and Kubo and Toyozawa[78] and multiphonon processes in solids. However, it seemed to us desirable to demonstrate this point for a simple model system which has many features in common with our model for the solvated electron in polar solvents.

(b) Changes of the force constants between the two excited states result in the distortion of the line shape from a symmetric form and lead to a temperature-dependent bond maximum.

(c) Anharmonicity effects are formally analogous to the change of force constants between the configuration diagrams which correspond to the two electronic states. To demonstrate this point, consider two anharmonic displaced energy surfaces

$$A(x) = \tfrac{1}{2}Kx^2 + wx^3, \quad \text{(A11)}$$
$$B(x) = \tfrac{1}{2}K'x^2 + w'(x+x_0)^3 + \bar{\alpha}. \quad \text{(A12)}$$

For the sake of simplicity, let us further assume that $K = K'$ and $w = w'$, whereupon

$$E(x) = 3wx_0x^2 + (Kx_0 + 3wx_0^2)x + h\nu, \quad \text{(A13)}$$

where now

$$h\nu = \bar{\alpha} + \tfrac{1}{2}Kx_0^2 + wx_0^3. \quad \text{(A14)}$$

For the case of physical interest $x_0 < 0$. We immediately notice from Eq. (A13) that the transition energy is equivalent for the case of two displaced surfaces characterized by different force constants [Eq. (A3)].

Thus the former formalism [Eqs. (A1)–(A10)] is directly applicable for the simple anharmonic model if we just replace $K'-K$ by $6wx_0$ and $K'x_0$ by $(kx_0 + 3wx_0^2)$ in all equations following Eq. (A4). If $K > |wx_M|$, we have for the temperature coefficient of the band maximum the value $+6k|wx_0|/K$. In this case $6wx_0$ may be larger than K so that an appreciable thermal shift of the band maximum may be observed. The asymmetry of the line shape can be inferred from similar arguments to those made in regard to Eq. (A10). We can therefore see that these results provide a direct link between thermal expansion of the cavity and the temperature dependence of $h\nu_{\max}$, as both are determined by anharmonicity effects.

While these model systems have pointed to three factors which can lead to asymmetric line shapes and temperature dependences of the absorption band, they do not agree with the experimental results or the theoretical calculations of Sec. VIII of this paper due to the neglect of the temperature dependence of $\bar{\alpha}$ and more general anharmonic distortions.

APPENDIX B: AN IMPROVED MODEL FOR THE ELECTRONIC ENERGY OF SOLVATED ELECTRONS

In the model described in Sec. IV of this paper we included the dipole potential only in the region up to the hard-core radius; see Eq. (17). A more accurate potential would consider that term up to the center of the dipole r_d:

$$V(r) = -N\mu e\langle\cos\theta\rangle/r_d^2 - \beta e^2/r_c, \qquad 0 < r < R$$
$$= -N\mu e\langle\cos\theta\rangle/r_d^2 - \beta e^2/r_c + V_0, \qquad R < r < r_d$$
$$= -\beta e^2/r + V_0, \qquad r_d < r,$$

where we assume V_0 acts in the entire region beyond the hard core. All notation is identical with that of Sec. IV. The results from this model (called Model 3) are listed in Table B. I and should be compared with Tables II and III. The numbers are very similar to those presented in the other model. The major change is that the $N=6$ cavities are slightly more stable, thus making the concept of a distribution of cavity sizes and other characteristics more likely. The $N=6$ cavities also have a slightly higher transition energy

TABLE B.I. Results of Model 3 for electrons in ammonia at 203°K.

V_0 (eV)	R_0 (Å)	E_{1s}	$E_t(R_0)$	$h\nu$	$\langle\cos\theta\rangle$	C_s
$N=4$						
2.0	1.85	−1.3108	−0.15061	1.7972	0.910	0.360
1.5	1.80	−1.6239	−0.46270	1.6351	0.901	0.317
1.0	1.75	−1.9630	−0.79851	1.4947	0.891	0.278
0.5	1.70	−2.3267	−1.15391	1.3751	0.880	0.242
0.0	1.70	−2.6679	−1.52494	1.2390	0.865	0.217
−0.5	1.65	−3.0695	−1.91077	1.1525	0.851	0.188
$N=6$						
2.0	2.30	−1.7950	−0.41657	1.9854	0.915	0.511
1.5	2.20	−2.0805	−0.65553	1.8327	0.911	0.459
1.0	2.20	−2.3105	−0.91708	1.6283	0.903	0.423
0.5	2.15	−2.6032	−1.20081	1.4716	0.895	0.379
0.0	2.15	−2.8674	−1.50540	1.2929	0.884	0.341
−0.5	2.10	−3.2027	−1.83220	1.1667	0.872	0.300
$N=8$						
2.0	2.85	−1.9968	−0.51074	1.8642	0.906	0.628
1.5	2.80	−2.1931	−0.68928	1.6927	0.902	0.588
1.0	2.80	−2.3639	−0.88679	1.4930	0.895	0.549
0.5	2.75	−2.5940	−1.10491	1.3289	0.888	0.501
0.0	2.75	−2.7965	−1.34726	1.1427	0.876	0.453
−0.5	2.75	−3.0158	−1.61482	0.9660	0.860	0.400
$N=12$						
2.0	3.45	−2.4108	−0.50525	1.6943	0.891	0.727
1.5	3.45	−2.5230	−0.64067	1.5302	0.887	0.699
1.0	3.40	−2.6921	−0.79039	1.3946	0.883	0.663
0.5	3.40	−2.8245	−0.95940	1.2293	0.876	0.624
0.0	3.45	−2.9181	−1.14500	1.0392	0.863	0.579
−0.5	3.35	−3.1781	−1.36643	0.9297	0.855	0.521

than $N=4$ cavities for the same V_0 and thus could contribute to a slightly asymmetric line shape, asymmetric on the high-energy side by a very small amount. The energy differences between the two models are in general small, and thus no new physically important information is obtained. It is presented here simply to indicate the insensitivity of our results to most details of the potential.

* This work is partially supported by a National Science Foundation Grant to Neil R. Kestner and an AFOSR Grant to J. Jortner. Computer time was supported primarily by National Science Foundation Grant to Louisiana State University.

† Alfred P Sloan Fellow.

[1] L. Onsager, *Modern Quantum Chemistry-Istanbul Lectures*, edited by O. Sinanoğlu (Academic, New York, 1966), Vol II, p. 129.
[2] G. Lapoutre and M. J. Sienko, *Metal Ammonia Solutions* (Benjamin, New York, 1964).
[3] J. C. Thompson, *Chemistry of Nonaqueous Solvents*, edited by J. J. Lagowski (Academic, New York, 1967), p. 265.
[4] J. L. Dye, Acct. Chem. Res. **1**, 306 (1968).
[5] F. Cafasso and B. R. Sundeim, J. Chem. Phys. **31**, 809 (1959).
[6] J. Eloranta and H. Linschitz, J. Chem. Phys. 2214 (1963).
[7] R. Catteral, P. L. Stodulski, and M. C. R. Symmons. J. Chem. Soc. **A437** (1968).
[8] Advan. Chem. Ser. **50**, (1964).
[9] J. W. Boag and E. J. Hart, J. Am. Chem. Soc. **84**, 4090 (1962).
[10] L. Keens, Nature **188**, 42 (1963).
[11] E. J. Hart, Science **146**, 19 (1964).
[12] L. M. Dorfman and M. S. Matheson, Progr. Reaction Kinetics **3**, 239 (1965).
[13] M. C. Sauer, S. Arai and L. M. Dorfman, J. Chem. Phys. **42**, 708 (1965).
[14] S. Arai and M. C. Sauer, J. Chem. Phys. **44**, 2297 (1966).
[15] M. F. Deigen, Zh. Eksp. Teor. Fiz. **26**, 300 (1954).
[16] A. S. Davydov. Zh. Eksp. Teor. Fiz. **18**, 913 (1948).
[17] J. Jortner, J. Chem. Phys. **30**, 839 (1959).
[18] L. Landau, Physik. Z. Soviet Union **3**, 664 (1933).
[19] J. Jortner, J. Chem. Phys. **27**, 823 (1957).
[20] D. E. O'Reilly, J. Chem. Phys. **41**, 3736 (1964).
[21] R. H. Land and D. E. O'Reilly, J. Chem. Phys. **46**, 4496 (1967).
[22] G. Careri, F. Scaramuzi, and J. O. Thomson, Nuovo Cimento **13**, 186 (1959).
[23] L. Meyer and F. Reif, Phys. Rev. **110**, 279 (1958); **119**, 1164 (1960); **123**, 727 (1961).
[24] J. Levine and T. M. Saunders, Phys. Rev. Letters **8**, 159 (1962).
[25] T. M. Sanders, Bull. Am. Phys. Soc. Ser. II **7**, 606 (1962); J. Levine, Ph.D. thesis, University of Minnesota, 1964 (unpublished); T. M. Sanders and J. Levine (unpublished).
[26] W. T. Sommer, Phys. Rev. Letters **12**, 271 (1964).
[27] M. A. Woolf and G. W. Rayfield, Phys. Rev. Letters **15**, 235 (1965).
[28] K. R. Atkins, Phys. Rev. **116**, 1399 (1959).
[29] G. Kuper, Phys. Rev. **122**, 1007 (1961).
[30] J. Jortner, N. R. Kestner, S. A. Rice, and M. H. Cohen, J. Chem. Phys. **43**, 2614 (1965); *Modern Quantum Chemistry—Istanbul Lectures*, edited by O. Sinanoğlu (Academic, New York, 1966), p. 129.

[31] K. Hiroike, N. R. Kestner, S. A. Rice, and J. Jortner, J. Chem. Phys. **43**, 2625 (1965).
[32] B. Burdick, Phys. Rev. Letters **14**, 11 (1965).
[33] B. E. Springett, M. H. Cohen, and J. Jortner, Phys. Rev. **159**, 183 (1957).
[34] R. C. Clark, Phys. Letters **16**, 42 (1965).
[35] L. Meyer, H. T. Davis, S. A. Rice, and R. J. Donnelly, Phys. Rev. **126**, 1925 (1962).
[36] H. Schnyders, S. A. Rice, and L. Meyer, Phys. Rev. Letters **15**, 187 (1965).
[37] H. Schnyders, S. A. Rice, and L. Meyer, Phys. Rev. **150**, 127 (1967).
[38] D. W. Awan, Proc. Phys. Soc. (London) **83**, 659 (1964).
[39] L. S. Miller, S. Howe, and W. E. Spear, Phys. Rev. **166**, 861 (1968).
[40] B. Halpern, J. Lekner, S. A. Rice, and R. Gomer, Phys. Rev. **156**, 351 (1967).
[41] J. Lekner, Phys. Rev. **158**, 130 (1967).
[42] B. Halpern and R. Gomer, J. Chem. Phys. **43**, 1069 (1968); **51**, 1031, 1048, 3043, 5709 (1969).
[43] B. E. Springett, M. H. Cohen, and J. Jortner, J. Chem. Phys. **48**, 2720 (1968).
[44] W. N. Lipscomb, J. Chem. Phys. **21**, 52 (1953).
[45] R. A. Ogg, Phys. Rev. **69**, 668 (1946).
[46] R. A. Stairs, J. Chem. Phys. **27**, 1431 (1957).
[47] D. E. O'Reilly, J. Chem. Phys. **35**, 1856 (1962).
[48] K. Iguchi, J. Chem. Phys. **48**, 1735 (1968).
[49] M. H. Cohen and J. C. Thompson, Advan. Phys. **17**, 857 (1968).
[50] J. Jortner and N. R. Kestner, in Metal–Ammonia Solns., Physicochem. Properties, Proc. Colloque Weyl II, Cornell Univ. 1969 (to be published).
[51] The reader should carefully note that our electronic energy in Eq. (26) is slightly inconsistent with our definition of V_0. In Eq. (27) we include contributions from the polarization of the medium but such effects were already included in the definition of V_0. This difference is minor since the charges are quite localized but in comparing V_0, which we use as an unknown parameter, with any direct measurement of it one must keep this slight difference in mind. The difference does not affect the ground state significantly but can affect the nature of the excited state, i.e., whether it is found or metastable. These points are being studied and will be reported in later publications.
[52] M. H. Cohen and J. Jortner, Phys. Rev. **180**, 238 (1969).
[53] This last point was emphasized by Professor L. Onsager in his comments at the Colloque Weyl II, Cornell University, June 1969. We are grateful to Professor Onsager for discussions on this problem.
[54] A. D. Buckingham, Discussions Faraday Soc. **24**, 151 (1967).
[55] See, for example, K. Iguchi, J. Chem. Phys. **48**, 1735 (1968). Here the orientation is considered from the viewpoint of a continuum model.
[56] D. Eisenberg and W. Kauzmann, *The Structure and Properties of Water* (Oxford U. P., New York, 1969), p. 46.
[57] R. F. W. Bader and G. A. Jones, J. Chem. Phys. **38**, 2791 (1963).
[58] U. Schindewolf, in Metal–Ammonia Solns., Physicochem. Properties, Proc. Colloque Weyl II, Cornell Univ., 1969 (to be published), and references discussed there.
[59] R. Catterall, in Metal–Ammonia Solns., Physicochem. Properties, Cornell University, 1969 (to be published), and references discussed there.
[60] See, for example, R. Catterall, in *Metal Ammonia Solutions*, edited by G. Lepoutre and M. J. Sienko (Benjamin, New York, 1964), pp. 41ff.
[61] This is based on preliminary unpublished calculations.
[62] H. Blades and J. W. Hodgins, Can. J. Chem. **83**, 411 (1955).
[63] R. K. Quinn and J. J. Lagowski, J. Phys. Chem. **73**, 2326 (1969).
[64] S. Golden and T. R. Tuttle, Jr., in Metal–Ammonia Solns., Physicochem. Properties, Colloque Weyl II, Cornell University, 1969 (to be published).
[65] W. R. Elliott, Science **157**, 559 (1967).
[66] See, for example, M. S. Matheson, Advan. Chem. Ser. **50**, 45 (1965).
[67] M. S. Matheson and L. M. Dorfman, *Pulse Radiolysis* (M. I. T. Press, Cambridge, Mass., 1969).
[68] M. C. Sauer, Jr., S. Arai, and L. M. Dorfman, J. Chem. Phys. **42**, 708 (1965).
[69] L. R. Dalton, J. L. Dye, E. M. Fielden, and E. J. Hart, J. Phys. Chem. **70**, 3358 (1966).
[70] R. R. Dewald and J. L. Dye, J. Phys. Chem. **68**, 121 (1964).
[71] D. A. Copeland and N. R. Kestner, preliminary results in Metal–Ammonia Solns., Physicochem. Properties, Proc. Colloque Weyl II, Cornell University, 1969 (to be published); complete results will be published in J. Chem. Phys.
[72] See, for example, M. Bixon and J. Jortner, J. Chem. Phys. **48**, 715 (1968); **50**, 3284 (1969) or K. F. Freed and J. Jortner, *ibid.* **50**, 2916 (1969).
[73] P. G. Varlashkin and A. T. Stewart, Phys. Rev. **148**, 459 (1966).
[74] P. G. Varlashkin and A. T. Stewart, *Positron Annihilation*, edited by A. T. Stewart and L. O. Roelling (Academic, New York, 1967), p. 313.
[75] P. G. Varlashkin, J. Chem. Phys. **49**, 3088 (1968).
[76] Such work is now in progress by P. G. Varlashkin, N. R. Kestner, and J. Jortner.
[77] M. Lax, J. Chem. Phys. **20**, 1752 (1952).
[78] R. Kubo and Y. Toyozawa, Progr. Theoret. Phys. (Kyoto) **13**, 161 (1955).